A Case study: Optimizing the district heating network of Amsterdam by implementing Thermal Storage

P.V.M van den Bent

July 2024 , Delft

MSc thesis in mechanical engineering

A Case study: Optimizing the district heating network of Amsterdam by implementing Thermal Energy Storage

Pepijn Vincent Maurits van den Bent

July 2024

A thesis submitted to the Delft University of Technology in partial fulfillment of the requirements for the degree of Master of Science in mechanical engineering

The work in this thesis is done in collaboration with:

VATTENFALL

Vattenfall Green Heat Strategy & Development
Vattenfall NV, Amsterdam

Supervisors:	Prof.dr. K. (Kamel) Hooman	(TU Delft)
	Prof.dr.ir. J.H. (Thijs) Vlugt	(TU Delft)
	ir. B. (Bart) Dehue	(Vattenfall)
	ing. C. (Casper) Jansen	(Vattenfall)

Confidentiality Statement

Some figures in this document are intentionally presented without y-axis labels to prevent the disclosure of sensitive information.

Author: Pepijn Vincent Maurits van den Bent
Date: Friday 28th June, 2024

Abstract

In the Dutch "Warmte transitie," district heating is set to play a predominant role, with the goal of achieving gas-free domestic heating by 2050. This necessitates upgrading traditional district heating networks to the fourth generation. To support this transition, the potential of decoupling heat production and demand through thermal storage is explored. A techno-economic case study on the district heating network of Amsterdam-East/Almere evaluates the value of heat storage. The literature study concludes that, given the current supply temperatures and financial objectives, heat should be stored as sensible pressurized heat. The transition period between 2030 and 2040 is modeled, focusing on shifting from fossil-based to power-to-heat-oriented district heating networks. A diverse asset configuration is implemented, providing affordable heat at low and medium electricity prices. The objective is to quantify the influence of thermal storage and its impact on asset dispatch dynamics. This study addresses a gap in the literature by providing a fundamental description of a diverse asset configuration transitioning towards a power-to-heat-based district heating network.

A numerical model using linear programming, specifically a combination of dual simplex and barrier methods, is employed. The main input variables are based on long-term commodity price forecasts. A rolling optimization horizon is implemented to focus on mid/short interval storage optimization, acknowledging the unrealistic nature of perfect forecasts. Non-linearity in the Combined Heat and Power (CHP) systems is managed by pre-defining state points within the operational domain. Additional constraints such as start-up costs, subsidies, and carbon taxes are included.

The correlation between increasing storage capacity and financial benefits appears logarithmic, primarily due to limited overcapacities in favorable power-to-heat assets. During the transition, the value of storage capacity diminishes due to rapidly decreasing operational costs, reducing the absolute value of Thermal Energy Storage (TES). Optimizing CHP dispatch generates significant value, attributed to its non-linear price formation. The transition shifts value generation from winter to summer months due to changes in overcapacity. The hybrid model, which optimizes both financial and environmental benefits, shows no significant decrease in carbon footprint but helps stabilize it while increasing financial gains, this is visualised with a Pareto front plot.

The new generation district heating networks with limited overcapacity can benefit significantly from small-scale heat storage capacity. For this specific network, an optimal storage capacity of 1600 *MWh* has been identified. Additionally, it is concluded that incorporating storage capacity enhances dispatch flexibility and provides resilience against future uncertainties.

Keywords: District heating, Fourth generation, Sensible heat storage, Linear programming, Power-to-heat

Acknowledgements

To start with, I want to thank my supervisors, Kamel and Thijs. If I can say so, it was quite a smooth ride. Thank you for allowing me to set my own path during my thesis. It had its ups and downs, but in the end, I learned by doing. Whenever I needed support, you were there to provide it. I was able to pursue my passion for researching on a macro level to benefit the energy transition, which led me to discover a new transition, the heat transition.

Therefore, I want to thank Casper and Bart from Vattenfall. It was really interesting to discuss results with you, and I learned a lot. I will continue my work in the heat sector, and I hope we will meet again soon.

From a peer point of view, I want to thank my housemate, Jelle. It was perfect to work on our theses at the same time, especially our meetings at ”Het Klooster.” I hope to drink many more pints with you.

Lastly, I want to thank my family for always supporting me throughout my life. Specifically, my dad—although we may have different opinions, I appreciate all of it. To my ever-loving mom, I hope you know I do too.

Finally, I want to dedicate my thesis to my grandfather. Not only during this thesis, but throughout my whole studies, he has been there for me. It felt like he was with me throughout the entire journey, celebrating the ups and downs. I want to say we did this together, and we will continue to do so.

Ad novam venturam

Contents

List of Figures

List of Tables

Acronyms

- CHP - Combined Heat and Power
- DHN - District Heating Network
- TES - Thermal Energy Storage
- EB - E-boiler
- HP - Heat Pump
- GEO - Geothermal
- BO - Boiler
- ETS - Emission Trading System
- FEM - Finite Element Method
- NGCC - Natural Gas Combined Cycle
- RE - Renewable Energy
- COP - Coefficient of Performance
- PQ-Diagram - Load scheme of combined heat and power plant
- P2H - Power to Heat
- C3PO - A model used by Vattenfall for simulating district heating networks
- P1, P2, P3 - Price levels or periods in pricing models
- VRE - Variable Renewable Energy
- LSTM - Long Short-Term Memory (a type of neural network)
- GEO - Geothermal
- H2 - Hydrogen
- CSP - Concentrated Solar Power
- LHTES - Latent Heat Thermal Energy Storage
- PCM - Phase Change Material

1 Introduction

1.1 Problem context

The Paris Agreement sets the ambitious goal of limiting global temperature increase to well below 2 degrees Celsius, with efforts to restrict it even further to 1.5 degrees. This means that CO_2 emissions have be reduced by 45% in the year 2030 and net zero in 2040 (United Nations [2015]). To achieve this objective a transition towards energy systems with reduced dependence on fossil fuels is needed, requiring significant technological advancements. Moving towards this goal, the increasing inter-connectivity of energy systems becomes evident, creating a demand for new optimization and integration strategies.

This study particularly emphasizes the connectivity of specific energy markets, namely exploring how the heat market interacts with the electricity market. The evolving catalog of supply and demand sources in these markets introduces dynamic fields that challenge traditional frameworks. To harness the full potential of renewable energy sources, innovative control mechanisms need to be implemented, and new ways of coupling supply and demand should be explored.

In Europe, nearly half of the energy consumption is allocated to heating and cooling, with residential heating accounting for over 36 % of the total demand (INTERNATIONAL ENERGY AGENCY [2012]). To address environmental concerns and reduce reliance on fossil fuels, the Dutch government has embarked on an ambitious initiative, named "van het gas af in 2050". By 2030, 1.5 million homes in the Netherlands will transition to being natural gas-free, with the ultimate goal of making all homes sustainable by the year 2050.

Currently, district heating covers 24 % of the heating demand in Europe, However, its prevalence is higher in countries with colder climates and urban dense areas, like northern Europe and metropolitans. However, as of 2021 in the Netherlands, the predominant sources of residential heat are gas-fired central heating units (around 77 %), with only 16 % supplied by heat pumps and 6.4 % by district heating (Statista [2021], CBS [2023]).

To successfully achieve the transition to sustainable heating, there is a need to increase the market share of both district heating and heat pumps. District heating, especially in densely populated urban areas, offers advantages such as efficient space utilization and support for large-scale geothermal projects. Nonetheless, challenges like high initial investment costs and heat loss pose significant obstacles to centralized heat production. District heating networks can be seen as a viable solution for distributing energy, particularly in the context of congested electricity grids (Tennet [2023]). For a successful energy transition, a balanced energy distribution system is and will be considered.

1.2 Research field

This research will delve into the increasing interconnection of the electricity and heat markets, proposing heat storage solutions to address intermittent effects. Furthermore, the study will be put to the test through a case study: The district heating network of Amsterdam-East/ Almere. This research will be conducted in collaboration with Vattenfall AB, one of Europe's major producers of heat and electricity. Specifically, the study will be carried out within the Green Heat Strategy & Development department at Vattenfall NV in the Netherlands. This newly established branch, located in Amsterdam, focuses on decarbonizing the Dutch district heating network operated by Vattenfall. The primary goal is to devise strategies for incorporating renewable heat sources. Vattenfall has committed to achieving net-zero emissions by 2040, including both its own power and heat production. This commitment introduces a compelling transitional phase characterized by changing heat sources.

As one of Europe's largest producers and distributors of district heating networks, Vattenfall serves metropolitan areas such as Amsterdam, and Uppsala. The district heating supply primarily relies on large combined heat and power plants (CHP). Vattenfall is planning a transition to utilizing industrial heat pumps in conjunction with geothermal energy, E-Boilers, and (seasonal) storage capacity. The long-term strategy also includes a shift to renewable fuels for combined heat and power (CHP) plants, such as bio-gas and hydrogen. Further exploring the potential of industry waste heat from waste treatment facilities and data centers. Lowering the supply and return temperatures, of the district heating network, to facilitate the integration of renewable energy is another aspect being investigated.

In 2022, Vattenfall's gas-fired power plants produced 10.4 *TWh*, and the number of heat consumers increased to 260 thousand equivalents, including both consumers and businesses in the Netherlands. The total heat sold amounted to 5.7 *PJ*, resulting in a reduction of 260,000 tons of CO2 emissions compared to 2021 (Vattenfall NV [2023]). In the Netherlands, electricity companies are required to publish the fuel mixes of the supplied electricity, Vattenfall achieved an increased renewability ratio of 62 %. The decision has been made to install a 150 *MW* Power-to-Heat boiler at the Diemen site, enabling the conversion of renewable-produced electricity into heat. Additionally, the Ministry of Economic Affairs and Climate has announced its intention for the mandatory public ownership of heat networks, significantly influencing future investment decisions and the implementation of new district heating projects.

1.3 problem definition

As explained in the previous section this study is fulfilled at the Green Heat Strategy & Development department at Vattenfall, the problem involves the optimization of a thermal energy storage (TES) capacity. This research is applied to a specific case, making it a case study. The optimization involves the district heating network of Amsterdam-East/Almere. This section aims to establish a fundamental understanding of the problem

To address the problem a better understanding of how the district heating network is supplied with heat is needed. As highlighted earlier different heat sources are implemented in the transition toward a fossil-free district heating network in 2040. Over the past few decades, this has been achieved mainly through the use of gas-fired combined heat and power (CHP) systems. However, in the upcoming decade, there is a clear shift toward a power-to-heat-based system.

The transition is detailed in Table 1.1, illustrating the gradual shift toward a fossil-free district heating network in Amsterdam. The primary load will be managed by the CHP plant, with plans to transition its fuel source to hydrogen by the year 2040. A 150 *MW* E-Boiler, expected to be completed by the end of 2024, will primarily operate during periods of low electricity prices due to its lower energy efficiency. The phased implementation of heat pumps and geothermal energy is in progress during the transition period. Finally, peak boilers are available, when operated gas-based they have a relatively high carbon intensity, therefore they will be fueled by hydrogen from 2040. Currently, there is a Thermal Energy Storage (TES) capacity in place, totaling 1600 *MWh*, with a discharge capacity of 400 *MW*. This storage capacity is primarily aimed at ensuring smooth asset operation and providing daily flexibility. On a typical winter day, the heat demand of the DH network ranges from 300-500 *MW*.

Table 1.1: Projected Thermal Power (*MW*) per Source Type

Year	**CHP** **(CH_4 /H_2)** (*MW*)	**E-boiler** (*MW*)	**Heat Pump** (*MW*)	**Geo-thermal** (*MW*)	**Boiler** **(CH_4 /H_2)** (*MW*)
2023	440	–	–	–	650
2030	440	150	31	30	650
2035	440	150	41	80	730
2040	260	150	101	100	800

Shifting to power-to-heat sources requires a clear understanding of how this impacts heat pricing. While gas prices remain stable during the day, electricity prices fluctuate due to real-time balancing between supply and demand, especially with the increasing use of renewable energy. Because of the low operational costs of renewable producers(approaching zero in some cases) the hours with cheap electricity will increase, this happens by following the merit order law (see section 3.1.2). This low price will enable power-to-heat assets to convert affordable renewable electricity into heat, for these periods an overcapacity of E-boilers is installed. On the other hand, when renewables are not available pricing peaks are expected. In this high electricity price regime, it will be undesirable to produce heat with CHP plants (while electricity production is sacrificed for the production of heat), as selling electricity to the grid at high prices becomes more lucrative. In between the pricing domain of the E-boiler and CHP, there is a grey area where it neither is interesting to dispatch either. The objective of this thesis is to assess whether the existing Thermal Energy Storage (TES) is optimal for the scenarios projected for the years 2030, 2035, and 2040.

While the peak capacities of the heat sources are provided in Table 1.1, it's important to note that they may not all operate for the same number of full load hours throughout the year. The right figure in 1.1 shows the load distribution during a year, this displays how many hours assets operate at a certain load, which correlates with the seasonal heat demand. With the annual operating hours on the horizontal axis and capacity in MW on the vertical axis. The base load is provided by heat pumps due to their favorable COP, their high CAPEX make them less attractive to cover the entire heat demand all year through. These are followed by waste heat from for example data centers. To fulfill the peak demand back-up boilers are installed, these are gas-fired. A secondary objective of the TES is to minimize the reliance on peak boilers during peak hours.

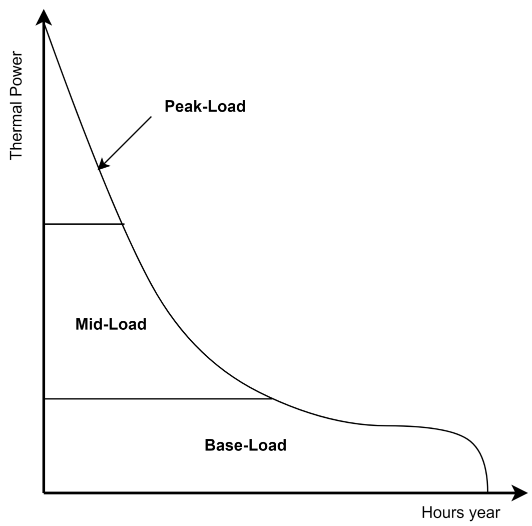

Figure 1.1: Load duration curve

1.4 Scope of work and research question

The objective of this study is to optimize the future district heating network of Amsterdam-East/Almere by integrating a thermal storage capacity (TES) alongside various heat sources. The optimization targets include achieving a minimum price for delivered heat and minimizing the carbon footprint associated with delivered heat. Special attention will be given to the combined heat and power (CHP) plant and an E-Boiler, chosen for their distinct pricing characteristics that offer optimization opportunities.

The study spans the period from 2030 to 2040, anticipating significant shifts in both the electricity and heat industries. Factors such as the interconnection between electricity and heat markets, the increasing share of renewable energy, volatility in electricity prices, intermittency, the Emission Trade System, and changes in fuel prices and types will be considered. The connection between the CHP plant, thermal energy storage, and their roles in the evolving landscape will be further investigated.

To support the decision for an ideal storage capacity, a numerical model will be developed. This model aims to provide a fundamental understanding of the dynamics among electricity prices, heat demand, heat storage, and heat sources, making use of a merit-order approach. It should explain the dynamics of decision-making regarding the implementation of storage and how the heating assets are dispatched. The model will be validated against state of the art models and will be subjected to sensitivity analyses. This model should be fast-converging and clearly highlight the results of different asset configurations and their effect on storage. Additionally, this study places a special focus on the transition towards a power-to-heat-based district heating network (DHN). Linear programming is proposed for optimization, focusing on storage capacity and charging/discharging benchmark prices as dependent variables. Furthermore, there is a desire for a universal model that can be easily implemented in district heating networks beyond Amsterdam.

The research scope is defined from a thermodynamic and economic point of view related to the district heating network. Heat sources will be modeled as sources, while end-users of heat will be treated as sinks. Hydraulic modeling of the district heating network and daily operational control will not be optimized in this study. Additionally, it's important to note that investment decisions will not be challenged in this study. Instead, the focus will be on optimizing Vattenfall's heat source strategy for the years 2030, 2035, and 2040. The study will specifically delve into aspects related to a long-term strategy for heat storage capacity. Moreover, Vattenfall will provide the necessary data for electricity prices, heat demand, carbon emission prices, and fuels within the study's timeframe.

The following research question is proposed to support the research objective:

How to develop a numerical model which optimizes the storage capacity integrated in the district heating network in Amsterdam-East/Almere ?

To answer the main research question a set of sub-questions is derived, they are provided below:

1. How will a growing storage capacity influence the reduced cost of delivered heat?
2. How will storage influence the dispatch of assets?
3. How will changing conditions over time influence the impact of storage?
4. How can financial and environmental benefits be optimized simultaneously?

1.5 Literature gap

District heating networks, traditionally studied for their thermodynamic and hydraulic models, optimization of conventional heat sources, and heat demand forecasts, now face new opportunities with the advent of fourth-generation district heating. This transition, driven by a growing share of renewable energy sources, is shifting the sector from fossil-based heating to power-to-heat solutions. The intermittent nature of renewable energy necessitates the use of thermal energy storage. While existing literature typically focuses on optimizing thermal storage with specific heat sources, this study uniquely examines the optimization of an E-Boiler and Combined Heat and Power (CHP) system integrated with thermal energy storage. This research aims to further investigate the transition of existing fossil-based district heating networks towards power-to-heat systems.

This approach hasn't been explored in existing literature, creating a notable gap. The study aims to fill this gap by examining the integration of an E-Boiler and CHP in district heating networks. It highlights developing optimization algorithms and control strategies to maximize efficiency, considering factors like variable electricity prices, heat demand fluctuations, and the intermittent availability of renewable energy. Additionally, the study explores selecting and optimizing thermal energy storage technologies and conducts economic and environmental assessments to evaluate the viability and sustainability of the proposed system. Applying the optimization framework to real-world case studies or simulations adds practical relevance, contributing valuable insights to the evolving landscape of fourth-generation district heating networks.

Furthermore, current studies on fourth-generation district heating networks (DHN) primarily focus on daily or seasonal storage. In this study, we will evaluate the mid-short storage timespan, ranging from one week to one month. This approach aims to bridge periods with limited renewable energy availability and maximize the utilization of days with excess renewable energy production. A hybrid multi-objective model will be integrated to further investigate the trade-offs between financial and environmental benefits.

To enhance the analysis, the techno-economic model will be complemented by a thermodynamic Finite Difference Method (FDM) model. This addition allows for the inclusion of energy losses and diffusion, establishing a connection between techno-economics and mechanical engineering aspects.

2 State of the art

To gain a more extensive understanding of the literature research problem, it is crucial to provide a comprehensive introduction to the current knowledge surrounding District Heating. This involves integrating insights from the latest developments at Vattenfall and highlighting emerging trends within the industry. This emphasizes the relevance of this study, it is underscored by the industry's dynamic shift toward power-to-heat applications. Vattenfall, with extensive experience in operating district heating networks, provides valuable insights, complemented by an analytical perspective and knowledge from the field of mechanical engineering. This chapter mainly describes the playing-field where this thesis is positioned.

2.1 District Heating

Approximately half of the energy consumption in Europe is allocated for heating purposes, and only 12% of this heat is currently derived from renewable sources (Abdur et al. [2018]). This highlights a substantial potential for decarbonizing the heating sector. While district heating is not a newly found solution, the focus of the latest generation is primarily on delivering fossil-free energy. Presently, the fourth generation of district heating networks is under development, emphasizing the integration of renewable energies.

Earlier generations concentrated on the integration of Combined Heat and Power (CHP) plants and refining control strategies to align supply with demand. Concurrently, advancements were made in the metallurgical aspects of piping and insulation. This third-generation district heating (DH) has evolved since the late 1970s and remains the predominant methodology worldwide. Typically, supply temperatures range from 70-120 degrees Celsius, with return temperatures at 40-76 degrees Celsius (Abdur et al. [2018]).

While the third generation of district heating has reached a mature stage, the fourth generation is currently an emerging technology. As of now, only pilot projects and small-scale setups have been initiated to explore its potential. A significant differentiating factor in these new district heating (DH) networks is the adoption of lower supply and return temperatures, aligning with the lower temperatures at which renewable heat sources become available. The integration of energy storage is also a key consideration, especially given the unpredictable nature of renewable sources.

The district heating network serves as a link between heat consumers and centralized producers, offering a range of potential heat suppliers.To date, Combined Heat and Power (CHP) plants play a prominent role, which generates both electricity and heat simultaneously. CHP plants operate with a high overall energetic efficiency and can be fueled with renewable fuels like hydrogen and biomass. A significant advantage of the district heating (DH) grid is its ability to distribute waste heat effectively, leveraging sources such as heat from waste-burning facilities and data centers. As stated earlier the storage of sensible or latent will also be implemented to further link the electric and heat grids. For instance, the excess electricity from intermittent renewables could be used to produce and store heat.

The district heating grid operates in various stages, each under different conditions. Initially, heat sources feed into the main distribution piping, operating at temperatures up to 120 degrees Celsius and a pressure of 1.5 *MPa*. Pumps are utilized to achieve the desired flow rate and overcome head losses. When it comes to losses, heat losses are more significant, ranging from 5 to 20% (Gong and Werner [2015]), whereas flow losses are in the range of 100-250 *Pa/m* (Skagestad and Mildenstein [2002]). On the other hand, fluctuations in the supply temperature can lead to a reduced lifetime of the insulation material inside the DH pipes (Vattenfall AB [2024]).

To regulate the transported heat capacity, two variables can be adjusted: the inlet temperature and the flow rate. Increasing both parameters subsequently raises pressure and heat losses. To enhance the grid's transport capabilities, it's beneficial to have high supply and low return temperatures, maximizing the amount of heat extracted from the network. For renewable sources, a lower supply temperature is preferable, but it poses challenges such as moisture and legionella, in addition to negatively affecting transport capability (Lund et al. [2014]).

The district heating grid and the end consumer can be connected either directly or indirectly. In the direct connection, the district heating network (DHN) is directly linked to the district heating grid. In the indirect setup, both are separated by a heat exchanger. The majority of connections fall into the second configuration. Indirect networks offer the flexibility to operate at different pressures and temperatures without affecting the building network. On the other hand, direct connections eliminate heat and head loss through the interconnected heat exchanger. Common types of heat exchangers include plate heat exchangers or shell & tube exchangers. From this interconnection point, heat enters houses or buildings, where tap water is heated by a heat exchanger. Typically, the heat is directly supplied to space heating through heat-emitting radiators.

3 Literature review

The literature review serves to outline the physical methodology forming the basis of the model. This chapter aims to provide a comprehensive understanding of district heating network operations and how these concepts can be translated into a fundamental model. Section 3.1 explains how the price of electricity is set. Given that pricing forecasts are a key input for the model, the paragraph explores how renewable energies contribute to pricing dynamics. It also discusses the impact on heat pricing and evaluates the forecasting implications. Additionally, it will introduce the European Emission Trading System (ETS).

Furthermore, the review will expand on heat producing assets and the distribution network (Section 3.3). The thermodynamic and hydraulic working principles will be evaluated to assist in determining the extent to which these parameters should be incorporated into the model (Section 3.3.6). Additionally, an in-depth exploration of various storage techniques will be provided. Here several storing techniques will be discussed, but also how to thermodynamically model a storage capacity with a finite element approach (Section 3.2). The last paragraph will focus on recent studies that delve into modeling district heating networks and assets. Various modeling and optimization techniques will be discussed, shedding light on advancements in the field (section 3.4).

3.1 Electricity

Since 2021, the European energy crisis has led to a surge in electricity prices, primarily driven by the sharp rise in gas prices induced by tensions between Europe and Russia (Zakeri et al. [2022]). Several factors are expected to shape the evolution of electricity wholesale prices in the long term. Fuel prices and the increasing CO_2 taxation will be key determinants of electricity prices in the years ahead. Trends, like the increasing share of RE's, suggest a decrease in wholesale prices at certain moments, primarily attributed to the merit-order effect. Renewable electricity sources, such as wind and solar, having both relatively low operational costs. Consequently, when these sources are available, they can effectively reduce the baseline price (Oosthuizen et al. [2021]). However, it's noteworthy that renewable energy sources (RE) largely depend on public schemes for support, and the final cost is also paid by the end consumer. The growing share of RE is transforming the dynamics of the traditional electricity system, driven by the intermittent and volatile nature of these sources. As non-dispatchable resources, REs significantly enhance the volatility of electricity prices. This shift also implies that conventional dispatchable energy sources , like thermal power plant, play a backup role during periods when REs are unavailable.

3.1.1 Pricing forecast

Distinguishing between short-term (typically day-ahead), mid-term (spanning months to several years), and long-term (ranging from years to decades) perspectives is crucial in understanding electricity market dynamics. Accurate short-term price forecasting holds immense significance for all participants in the electricity market. The day-ahead market sets the price for the upcoming day. Power suppliers, such as Combined Heat and Power (CHP) plants, use day-ahead forecasting to optimize bidding strategies, while power consumers use this in planning their operational strategies. Long-term forecasts help stakeholders in making investment decisions over extended periods. The increasing integration of renewable energy sources adds complexity to price forecasting, and the growing connection of power markets further complicates pricing predictions (Bhatia et al. [2021]).

Various methods are employed to predict day-ahead pricing forecasts, ranging from statistical autoregression models to machine learning techniques (Meng et al. [2022]). Given the complex nature of electricity price formation, a common approach involves using hybrid models that integrate various methods. In a study by Meng et al. [2022], the focus is on predicting prices for a system with a high penetration of renewables, such as wind and solar. The prediction model relies on an attention mechanism-based Long Short-Term Memory (LSTM) hybrid prediction, and it is trained on datasets from the Danish electricity market.

Econometric models are overall capable of predicting short-term pricing forecasts but have difficulty with a longer time horizon. This is because statical models rely on assumptions that can be changed over time by political and technological transformations. When you move to medium-term forecasting, up to a year, the seasonable variation becomes important. For example, Martin-Rodriguez and Caceres-Henandez study the hourly Spanish electricity demand by applying periodic cubic splines to describe seasonal and weekly variations (Martín-Rodríguez and Cáceres-Hernández). Here the key difficulty lies in transforming seasonal fluctuations in supply and demand into hourly profiles. Long-term pricing forecasts are not commonly accessible due to their economic value. Vattenfall will supply electricity pricing forecasts in the hourly domain throughout the designated time span of 2030 to 2040. It's essential to recognize that as the forecasting horizon extends, uncertainty naturally increases. Consequently, sensitivity analyses are conducted on the model to assess its responsiveness to varying factors. This practice helps in building the robustness and reliability of long-term pricing predictions, considering the dynamic and evolving nature of economic and market conditions over an extended timeframe.

3.1.2 Influence of renewable energies on electricity prices

The increasing share of renewable energies has resulted in heightened price volatility in the day-ahead market. It is crucial to distinguish between positive and negative price spikes, particularly concerning their timing. Negative prices tend to occur predominantly during nighttime hours when demand is low, coupled with an excess of wind power availability. Conversely, positive spikes are associated with increased demand, decreased supply, and typically arise during morning and afternoon peak periods. The growing share of renewable energies in the overall energy system increases the likelihood of encountering price peaks. Notably, wind power plays a significant role in driving the occurrence of negative price events, making it a key factor in this context (Hagfors et al. [2016]).

Electricity, as a unique commodity, has the distinct characteristic of being produced and consumed simultaneously. During periods of scarcity and increased demand, producers with available capacity hold market power, allowing them to set prices significantly above marginal costs, leading to the formation of exceptionally high prices. (Bunn et al. [2016]). Conversely, an excess of supply can lead to negative pricing peaks. At any given moment, various supplying producers operate at different pricing levels. The bidding price for conventional fossil-based energy, for instance, is heavily influenced by fuel prices. Until recently the producers consisted mainly of dispatchable producers going from relatively cheap nuclear and coal up to the most expensive peak load producers gas and oil (Figure 3.1). The emergence of renewable energy sources with low operational costs has replaced the baseload of conventional plants when available.

The supply side is structured by the Merit Order (MO) Curve (refer to Figure 3.1). This curve aligns power demand with the merit order, establishing the price that each producer receives. In other words, all producers receive the bid of the highest bidder, which is set. Depending on the demand, the lowest possible settling price is determined. When renewable suppliers are unavailable, prices increase. In scenarios where renewable energy is abundant, the prices of electricity can be shaped by consumers with flexible demand, such as large electrolyzers and E-boilers, leading to higher electricity prices. As a result of an increasing stake of renewable energies, conventional power plants undergo a reduction in operational hours. For instance, a Combined Cycle Gas Turbine (CCGT) plant in Spain experienced a decline from over 4000 hours in 2008 to less than 1000 hours in 2014. Despite fixed investment and operational and maintenance costs, these plants remain essential for providing flexibility to the electricity grid (Pariente-David). In the future, a mechanism for dispatchable flexibility will become increasingly relevant. This transition pushes conventional power plants further up the right side of the merit order curve, as illustrated in Figure 3.1.

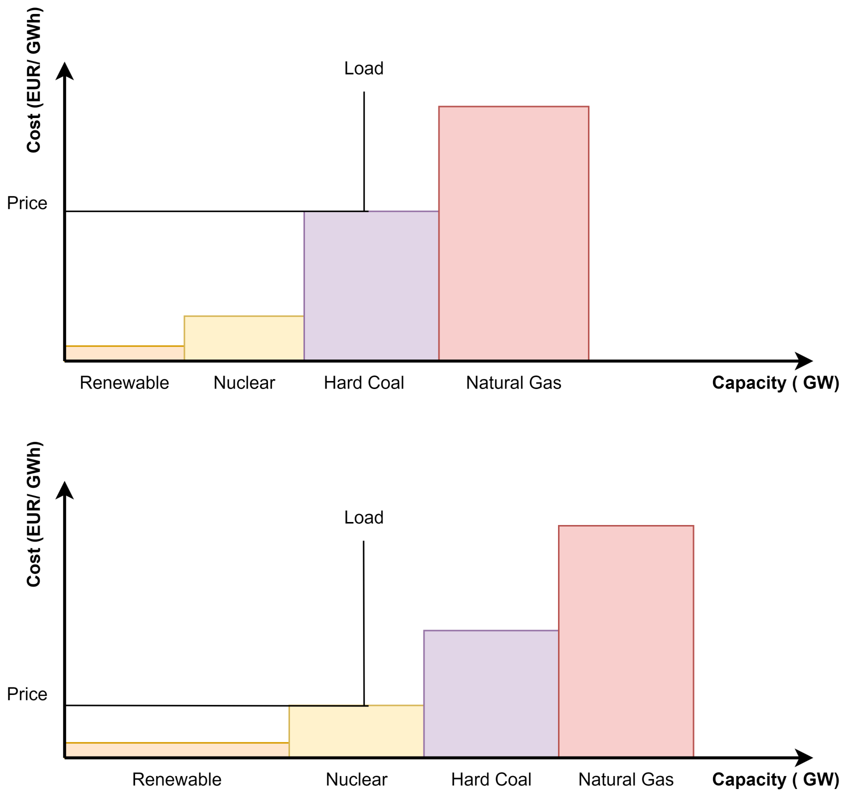

Figure 3.1: Merit Order bidding ladder mechanism

3.1.3 Pricing of heat

One of the primary goals in optimizing the district heating network is to provide affordable heat for domestic use. With the electrification of heat sources the electricity price plays a dominant role in setting the price of heat, on the other hand, fuel prices and carbon taxation have a significant influence on the overall price of heat. Assets that generate both heat and electricity concurrently benefit from higher electricity prices, enabling them to sell surplus electricity back to the grid. However, it becomes economically impractical to prioritize heat production over electricity in such cases. In section 3.1.2 the merit order is explained for electricity pricing, this can also be done for the marginal price of heat. The marginal prices of heat will be used as an input for the model.

To further analyze the marginal costs of heat it is useful to illustrate their relationship between the electricity pricing. The four assets included in the case study and their marginal costs are discussed below. The derivation of the marginal cost is formulated in equation 3.1. The marginal cost is the differential function of the cost with regard to the heat produced (Q), C_{input} the cost of energy input and C_{CO2} the cost of emission rights. $C_{O\&M}$ implies the variable operation and maintenance cost and $r_{electricity}$ is the missed revenue for not selling electricity to the grid or selling electricity below the marginal cost of electricity (in the case of the combined heat and power plant).

$$MC(Q) = \frac{d(C_{input} + C_{CO2} + C_{O\&M} + r_{electricity})}{dQ} \tag{3.1}$$

- **CHP**
  Combined heat and power plant can produce heat and electricity simultaneously, extraction CHP's can be operated at different power-to-heat ratio's, In this paper the revenue streams of heat and power are seen as two separated commodities. The plant has as input costs: fuel, CO_2 tax and O&M. When the plant is operating below this equivalent electricity price a loss is made in terms of electricity revenue. When the plant is producing heat above this benchmark it would be more economical to switch to power only operations. In the time span from 2030 till 2040 the CHP is expected to change its fuel to hydrogen.
- **E-Boiler**
  Electrical boilers will take over the role of conventional boilers is the further, the main difference is that they are dependent on electricity prices. These boilers operate on the basis of resistant heating and therefore operate with an efficiency of 99% (COP of 1).
- **Heat Pump**
  As discussed before the heat pumps will cover the base-load of the heat demand, the price of heat mainly depends on the electricity price and the COP. The COP is dependent on the source temperature (potentially geothermal) and for industrial heat pumps this is around 3.6 (Bert den Ouden [2017]).
- **Boiler**
  The gas-fired boilers are called peak assets because they are operated in peak hours, while the carbon intensity of this way of heating their use is to be minimized. The marginal costs are directly linked to the price of natural gas, which makes them independent from the electricity market. In the transition period from 2030 to 2040 the fuel of these boilers will be changed from natural gas to green hydrogen.
- **External heat**
  Additional heat can also be bought by external parties, for instance from data centers and waste treatment facilities. The price depends on the contract made between the DHN operator and the external party. In some cases, utilizing excess heat can be offered as a service. For example, for data centers, this could potentially serve as an additional source of revenue.

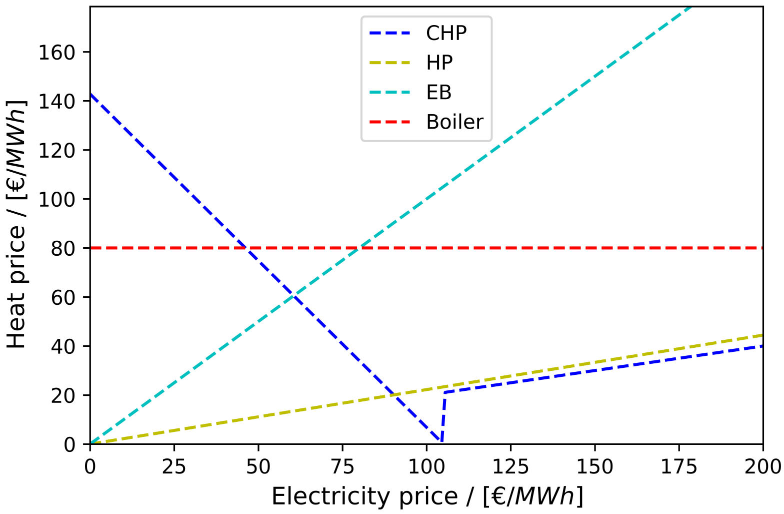

Figure 3.2: Marginal costs of heat in relation with electricity price

To illustrate the relationship between the electricity price and marginal costs, an example is provided in Figure 3.2, showing different assets and how the heat price correlates to the price of heat. It's worth noting that a fixed power-to-heat ratio is applied here, and the marginal cost of power and heat production is combined, which deviates from the methodology of this study. For the gas boiler, a price of €25/MWh and a carbon price of €60/MWh is considered Gonzalez-Salazar et al. [2023]. For the Gas turbine, a thermal efficiency of 52% and a constant power-to-heat ratio of 0.7 is assumed. The Natural Gas Combined Cycle (NGCC) has a thermal efficiency of 40%, and the power-to-heat ratio is set to 1.2 as a constant.

3.1.4 Emission trading system

In 2005, Europe implemented the European Emission Trading System (ETS) as a market instrument to curtail greenhouse gas emissions. This system operates with a capped amount of polluting emissions (measured in million metric tons per year), gradually reducing these emission allowances each year from 2005 onward. The ETS restricts the volume of emitted CO2 from large installations, particularly those exceeding a heat excess of 20 MW, primarily power plants and carbon-intensive industries. During the initial phase of the ETS, these emission allowances were allocated for free instead of being auctioned. Following phases saw an increase in the proportion of bonds auctioned, reaching approximately 60% in 2013 and growing thereafter to almost all bonds in 2020 (European Comission [2008]). Yearly allocations of emission allowances to installations have been decreasing, aiming to progressively reduce greenhouse gas emissions. This approach introduces an economic trade-off wherein installations can opt to cut emissions or purchase additional emission allowances on the ETS. Conversely, if an installation emits less than its allowance, surplus bonds can be sold on the ETS. This mechanism facilitates a cost-effective reduction of emissions without extensive government intervention. In 2021, auctioned bond prices settled around $50, and the European Commission has projected an increase to $140 per bond in 2030 (Dan Williams [2021]). Currently, emission bonds are traded at approximately €60/t, with forecasts indicating a steady increase from 2030 to 2040. Post-2040, bond prices are expected to surge due to approaching net-zero goals. A graphical representation of this forecast is provided in Figure 3.3. The given price is in euros per ton of carbon dioxide (€/tonne). For natural gas, each megawatt-hour of energy produced results in emitting 201.96 kilograms of carbon dioxide (kg/MWh) (Our World in Data [2023])

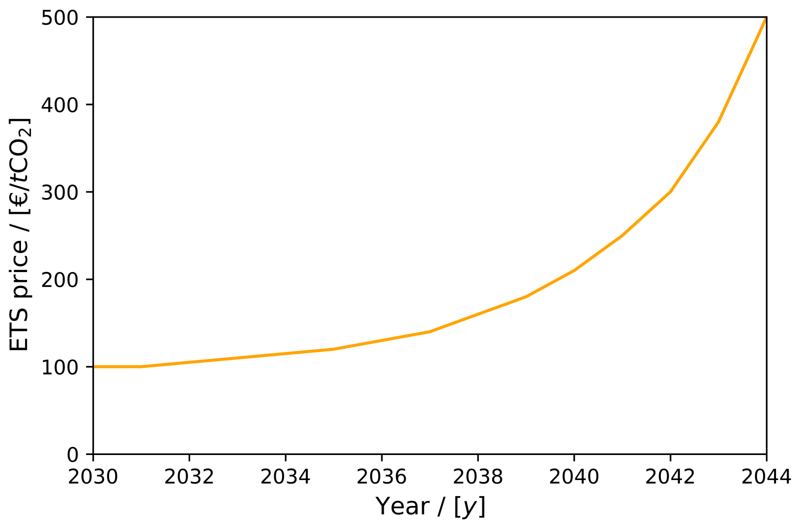

Figure 3.3: Forecast CO_2 ETF price evolution (Gabin Mantulet [2023])

3.2 Storage

With the recent changes in the energy markets, which are described in 3.1, and in particular the growing variation in electricity prices during the day, a necessity for balancing measures is created. Thermal heat storage could fulfill this role and ensure a stable price of heat in a volatile market. Within the scope of the fourth-generation district heating networks, much literature is dedicated to integrating heat storage into the district heating system. There are several possibilities to fulfill this need for stability, duration and storage method are the two most distinctive factors. Options range from seasonal to diurnal heat storage, encompassing sensible and latent heat storage. Additionally, chemical heat storage is also considered. Within the district heating system storage possibilities occur, using the thermal inertia of consumer and distribution assets (Le Sko et al. [2018]). Different storage systems will be evaluated on their maturity, economical feasibility, and temperature application range.

There are two types of timescales for storing thermal heat in a DHN: diurnal storage and seasonal storage. Diurnal storage addresses the daily fluctuations in heat demand (see figure 3.4), allowing for the smoothing out of heat demand over an extended period. This integration of thermal storage not only supports a more consistent heat demand profile but also enables electricity-driven assets to maximize their output during periods of favorable electricity prices. For example, thermal storage can be dispatched during weekends when electricity prices are typically lower on average. Moreover, it offers the potential to reduce dependence on peak boilers by discharging stored heat when demand is high.

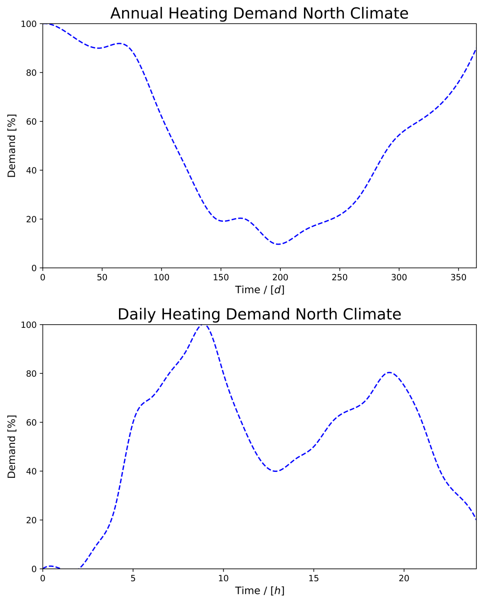

Figure 3.4: Load curves for north climate (Guelpa and Verda [2019]
)

On the other hand, seasonal storage addresses the broader mismatch between low heat demand in deep summer and high demand in the winter. Excess renewable or waste energy can be stored during periods of abundance to meet the elevated demands during the winter season. Challenges associated with integrating Thermal Energy Storage (TES) systems with district heating include the upfront investment costs and thermal energy losses.

3.2.1 Sensible heat storage

Sensible heat storage is a widely used storage method for daily short-term storage in combination with a DH network. The fundamental principle involves shifting the storage temperature without changing the phase of the medium. Water is the most commonly used medium for sensible heat storage, given its favorable physical properties, such as density, specific heat capacity, and thermal conductivity. However, other materials with suitable physical characteristics can be used as well. A method in finding a suitable storage medium is further described in Fernandez et al. [2010], in this temperature domain water is proposed as medium due to its widespread availability and relatively low costs.

A water-based Thermal Energy Storage (TES) system operates by storing water at different temperature levels without mixing. Within the system, a thermal separation layer known as a ”thermocline” is established between the hot and cold levels. The thermocline is characterized by a temperature gradient that transitions from the bottom to the top, typically with a thickness of approximately 1 meter. The method used to maintain the separation of hot water from cold water is called ”stratification”.During the charging phase, hot water is supplied at the top from the supply line of the District Heating (DH) network. Simultaneously, cold water is drawn from the bottom and directed into the return line from the DHN. This method allows for the alteration of the stored energy with a constant mass of water. To prevent turbulence-induced mixing, diffusers are strategically installed within the system. This stratification technique enables the efficient storage of thermal energy at different temperature levels in the water-based TES system. A method of describing the thermocline in a 1-D manner is given by Cruickshank and Baldwin [2022], here man makes use of the so-called ”node method”.

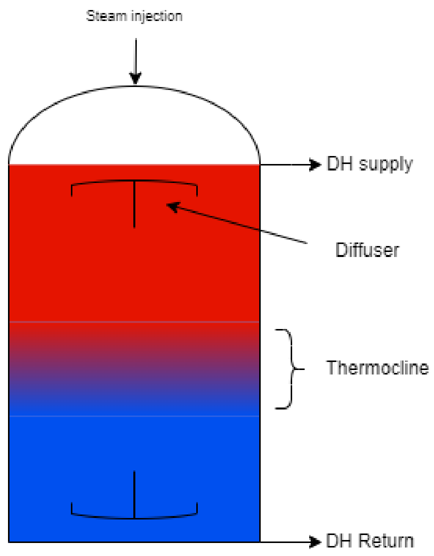

Figure 3.5: General layout thermal storage tank

There are two types of tank storage: pressurized and atmospheric, pressurized storage is necessary when storage temperatures exceed 100 C° to prevent water from vaporizing. An additional advantage of storing heat under pressure is the elimination of the need for extra pumps, as the pressure difference with the District Heating (DH) network is sufficient for circulation. The maximal storage capacity in a tank is determined by the temperature span, making it desirable to have as large a temperature difference as possible. In pressurized systems, the temperature span can be as high as 50-55 C°, which is mainly dependent on the supply and return temperatures of the DH network (Thomsen and Overbye [2016]).

For short-term thermal storage, cylindrical tanks are the predominant method, with literature suggesting storage capacities ranging from 10-100 m^3. This study aims to assess whether these capacities remain suitable in the context of the years 2030 to 2040. An optimization approach is applied to minimize surface area and, consequently, thermal losses by establishing an optimal ratio between the height and radius. Research by Dahash et al. [2017] suggests that the height should be double the radius to achieve minimal surface area and maximize volume, thereby improving the efficiency of the storage system.

The energy stored in the tank is described by equation 3.2. A detailed understanding of the stratification layer within the tank is crucial for accurate modeling. Li et al. [2021] provides a numerical approach to describe the stratification process. To further minimize heat losses, an insulation layer of 0.1 *m* polystyrene is applied, featuring a thermal conductivity of 0.03 *W/m.K*. Thermal losses typically constitute up to 5% in short-term thermal storage systems, while the capital expenditure (CAPEX) ranges from 30-50 Euro per cubic meter (Guelpa and Verda [2019]). These considerations play a vital role in optimizing the efficiency and cost-effectiveness of short-term thermal storage solutions, particularly in the context of next-generation district heating.

$$E = m \int_{T_1}^{T_2} c_p(T) \cdot dT \tag{3.2}$$

In addition to tank sensible heat storage, pits can also be utilized to store sensible heat. In this method, the storage capacity is buried in the ground and insulated with a plastic coating, leveraging the "Thermocline" principle. A key factor in this approach is the calculation of heat loss, where the thermal conductivity of the ground plays a crucial role. Groundwater can also impact thermal performance, and in the literature, pit storage is frequently examined within the context of seasonal heat storage.

For seasonal heat storage, three common techniques are tank-pit storage, aquifer storage, and borehole heat exchangers. Thermal losses in these systems can be significant, reaching up to 30% (Xu et al. [2013]). Due to these losses, auxiliary heat sources such as heat pumps are often required. Furthermore, the flexibility of these systems is limited by their thermal inertia and operational principles. To narrow the scope of this study, aquifers and borehole heat exchangers will not be further elaborated.

3.2.2 Latent heat storage

Latent heat storage utilizes the energy required to change a material's phase, this process takes place at a constant temperature. Material selection for latent heat storage is primarily based on phase change characteristics and thermal conductivity. There are two interesting groups of Phase Change Materials (PCMs): organic and inorganic. The melting temperature is a key parameter as it determines the operating temperature of the system.

Among organic PCMs, paraffin wax is a matured technology with a melting temperature ranging from 90K to 388K, providing a moderate storage density of 150 MJ/m^3. also, the low thermal conductivity of organic PCMs can result in lower (dis)charging rates (Jayathunga et al. [2023]). Non-organic salt hydrates are a promising storage technology, having double the volumetric latent storage capacity (350 MJ/m^3). The limiting factor for district heating applications is the melting temperature, which ranges from 250°C to 1680°C.

Literature suggests that latent heat storage is more suitable for district cooling applications due to the lower temperature difference between supply and return temperatures. In the context of low-temperature district heating networks, a study by J.F.C. Flores [2017] found that latent heat storage is generally four times more expensive than sensible heat storage. However, by lowering the supply and return temperatures to 50°C and 60°C, respectively, this cost difference reduces to 1.5 times.

3.2.3 Chemical energy storage

Thermal energy can be stored in the form of chemical energy, and this can be broadly categorized into two main sections. Firstly, there are chemical reversible endothermic reactions that can be triggered when excess heat is available. The products of these reactions can be stored at ambient temperature, and when heat is needed, the reverse reaction can be employed. Secondly, absorption and adsorption occur when a gas bonds to the surface of a solid. Chemical storage can reach a storage density up to 400 MJ/m^3 (where sensible heat storage stores 200 MJ/m^3 with a temperature difference of 50 $C°$) (N'Tsoukpoe et al. [2009]). While the chemical energy is stored at ambient temperature heat loss plays not a predominant role. Figure 3.1 displays all literature of chemical energy storage in combination with district heating applications, it can be seen that there are some challenges to overcome with the economical being the most severe, additionally the operating temperatures are not in line with the supply temperature of a DHN.

Table 3.1: Comparison of different substances for thermal storage (Guelpa and Verda [2019])

Substance	**Phenomenon**	**Outcomes**
$NaOH/H_2O$	Sorption	The system is feasible, heat storage density from 3 to 6 times higher than water depending on the application
$LiCl/H_2O$	Absorption	Commercialized but high cost of the material (not suitable for seasonal storage)
$MgCl_2/H_2O$	Absorption	Significant storage density with an economic material
$NaOH/H_2O$	Absorption	The absorption occurs much slower than expected
Zeolite (open)	Adsorption	Feasible but low discharge rate, better with high temperature
$Silica/H_2O$	Adsorption	Not feasible for long term because of low heat storage density
AQSOA FAM Z02/water	Adsorption	Heat/cold and daily/seasonal tests in various operating conditions. Performances highly influenced by the working conditions. It reaches a storage density 5 times the water.
$Zeolite/H_2O$	Adsorption	Flow rate has a low effect on results. Moisture strongly affects results. Performances do not depend on the number of cycles

3.2.4 Conclusion

In this chapter, three different storage techniques have been introduced. While the primary goals of this study are economic and environmental, it can be stated that sensible heat storage is the most predominantly chosen. This is mainly because its operating temperatures align with those of the district heating network. The hypothesis is that short-term storage will be the outcome of this study, where heat loss is not a decisive parameter. Additionally, the case is not situated in a densely urban environment, partly diminishing the advantage of a denser storage capacity. If the hypothesis is proven wrong by the results of the study, this consideration will be revisited.

3.3 Heat and power

3.3.1 Combined power heat plant (CHP)

In the scope of this thesis, one combined heat and power (CHP) is integrated into a district heating (DH) network. This plant co-generates heat and electricity simultaneously, which can improve energy production efficiency (Akorede et al. [2010]). Conventional power plants transform around 55 % of the fuel into usable energy, the majority of this energy is lost in the form of waste heat. By combining the power and heat generation the energy efficiency can be improved to 80 % (Mago et al. [2009]). There are two types of CHP plants, first back-pressure plants, here the electricity versus heat ratio is fixed, heat is extracted after the last turbine stage. Secondly steam extraction turbines, these have a greater flexibility concerning the heat ratio, steam is extracted between turbine stages and all steam can be condensed to generate electricity. There are two operating strategies an extraction CHP can be dispached. First full co-generation mode, hereby maximum heat recovery is fulfilled. It can be said that hereby some of the electricity generation is sacrificed to produce heat, the heat loss ratio is approximated to be 1 *MW* of electricity production could be 4 *MW* of heat (Michael Goll [2017]). The second mode is the full condensing mode, here no steam is extracted but all steam is condensed to a maximum, this means no usable waste heat is generated.

In the heat network analyzed in Amsterdam-East/ Almere a natural gas-fired combined cycle gas turbine with steam extraction is installed. A quick understanding of all components installed in a CHP is provided. A schematic overview can be seen in 3.6, starting with a gas turbine which consists of a compressor and turbine. The compressor compresses air and is then led to the fuel chamber, where it is mixed with fuel and ignited. The air is expanded in the turbine which is connected to a generator, the exhaust gas is led through the heat recovery system which fed the secondary cycle. In this cycle the medium is steam, the steam is heated by the heat recovery system and compressed. First, the steam is lead through the high-pressure turbine, then it is re-heated again in the heat recovery system. Now the steam expands through the intermediate/low-pressure turbines, it can be seen that after the intermediate turbine steam is extracted and fed to the DH network. Finally, both streams are condensate in the condenser, this happens at a near-vacuum.

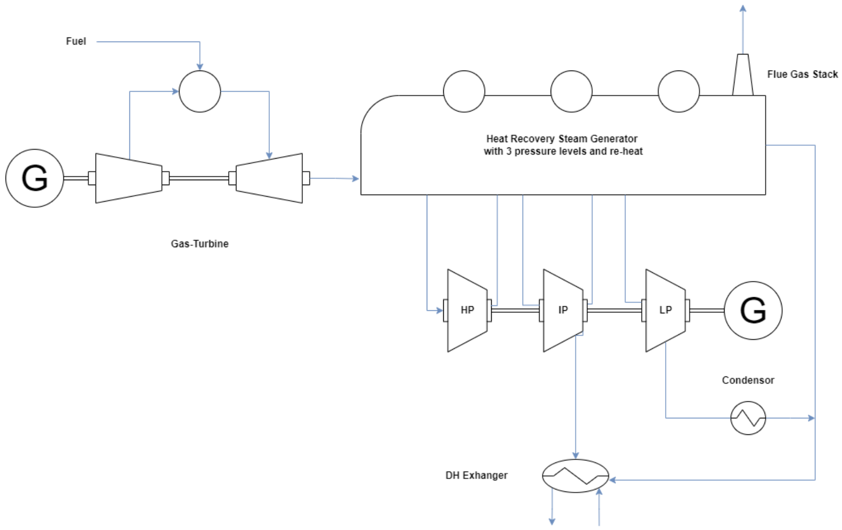

Figure 3.6: Schematic PGU flowchart

To address the different operating states of the CHP a few operating parameters will be introduced, first the energy can be divided into energy produced while operating in combined heat and power mode. E_{CHP} is the electricity produced in combination with useful heat, while $E_{non-CHP}$ is the part where no heat produced aside electricity production, combined they will give the total amount of electricity produced (E_{total}). This same distinguishing can be made with other parameters like fuel usage. One of the main reasons for making this split-off is to calculate the overall efficiency. The full condensing load efficiency is described in 3.3, here β stands for the heat loss ratio (approx. 0.25 Michael Goll [2017]). Changing efficiencies can be challenging, Milan et al. found a non-linear way to describe the thermal efficiency of a CHP. The next characteristic value of a CHP plant is the power-to-heat ratio (C),this represents the ratio between electricity and heat during maximal co-generation. Further derivation of the C value is displayed in equation 3.3, for steam extraction plants 0.45 is a widely used value Michael Goll [2017].

$$\eta_{non-CHP-E} = \frac{E_{Total} + \beta \cdot H_{CHP}}{F_{CHP_u}nit} \qquad C = \frac{E_{CHP}}{H_{CHP}} \tag{3.3}$$

The Combined Heat and Power (CHP) system offers flexibility in its operating states, determined by the power versus heat ratio as depicted in figure 3.7. The graph also provides insight into the heat loss ratio, derived from the slope coefficient of line **A-B**. Operating modes include the electricity-only mode (full condensing), where the system runs to fulfill heat demand even in unfavorable electricity price scenarios, operating in a minimum fuel mode to minimize losses. On the other hand, during periods of favorable electricity prices, the system maximizes electricity production. Full cogeneration mode, marked by maximal heat extraction and electricity production (line **B-C**), is another operational state. The system's efficiency varies with different load levels, with full-electric plants typically achieving efficiencies between 49-62 %, whereas concentration efficiencies around 80 % are attainable

(Koç et al. [2020]).The model will obtain efficiency data at various load levels from the operational records of Vattenfall. One thing to take into account is that the CHP units are not only active on the day-ahead market but also provide balancing services to the grid, while this market tends to have a more unpredictable behavior. In the year 2023, for instance, the CHP operated for approximately 6000 full load hours, encompassing both heat and electricity production, as well as balancing (Vattenfall AB [2024]).

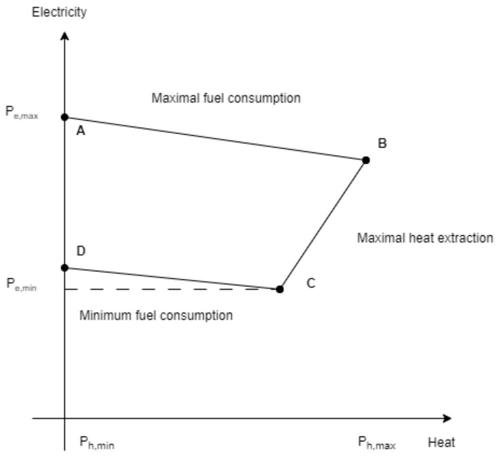

Figure 3.7: Feasible Operation Region of combined heat and power plant

3.3.2 Cycling of a power plant

As variable renewable energy sources increase, traditional electricity producers face challenges in adapting their operating flexibility. While fossil-fuel-based plants were accustomed to operating at constant load levels, Combined Heat and Power (CHP) plants offer flexibility but not without consequences on their lifespan and Operation & Maintenance costs (O&M). Operating these assets in a flexible manner, involving frequent cycling of ”on and off” states, introduces thermal and pressure stresses that can lead to damage mechanisms such as creep-fatigue. This dynamic loading induces shorter life expectancies, highlighting the importance of understanding the increased costs and their impact on the plant's lifespan, which should be integrated into the model. Additionally, the ramp rates will be evaluated to provide a realistic dispatching strategy for the CHP unit.

To achieve this, we refer to the report ”Power Plant Cycling Costs” produced by Intertek APTECH, which specifically describes the influence of renewable energies on conventional power plants (Kumar et al. [2012]). Also Brouwer et al. [2015] is used,both results align with Vattenfall's operational data. The combined gas and steam turbine are considered in series. While the gas turbine has a relatively fast response time, some time is needed for the steam turbine to reach the set load condition (Decoussemaeker [2016]). The following states of the CHP are defined: hot (offline for $\leq$ 12 h), warm (offline for 12–72 h), and cold (offline for $\geq$ 72 h) starts, with startup costs mainly applicable after periods of non-operation.

Table 3.2: Flexibility parameters natural gas combined cycle (Brouwer et al. [2015])

Ramp rate (%/min)	Start-up time (h)			Start-up cost (€/$MW_{installed}$)		
	Hot start	Warm Start	Cold start	Hot start	Warm Start	Cold start
6 ± 2	$1 \pm \frac{1}{2}$	$2 \pm \frac{1}{2}$	3 ± 1	27 ± 11	39 ± 20	57 ± 29

Table 3.2 presents various parameters related to the dynamic behavior and cost of a CHP plant, differentiated by state-of-the-art parameters per decade. Hot, warm, and cold start distinctions are made, with startup costs particularly relevant after periods of non-operation. Additionally, Brouwer et al. [2015] fitted a non-linear function to the partial load efficiency. Load cycling accelerates damage to many components, translating into Equipment Forced Outage Rates (EFOR). For instance, a cold start increases the EFOR by 0.0037 % per full cycle. For further insights into the effects of load cycling, please refer to Kumar et al. [2012].

3.3.3 Hydrogen fired CHP

Vattenfall aims to be carbon-free by 2040 by converting its combined heat and power (CHP) plants to use hydrogen in internal combustion engines. Hydrogen has a high energy mass density, about three times more than diesel (Yu et al. [2023]). However, retrofitting poses challenges like increased combustion speed and temperature, leading to issues like abnormal combustion and higher nitrogen emissions. To address this, hydrogen can be blended with traditional fuels, with the current common blend being 30 %, and a preferred limit of 50 % hydrogen.

The shift to hydrogen affects key parameters, such as thermal efficiency and fuel consumption. Implementing hydrogen as the primary fuel can enhance the thermal efficiency of internal combustion engines (ICE), leading to lower fuel consumption. The efficiency of the combined steam cycle is not influenced by this change (Koç et al. [2020]). Green hydrogen presently costs roughly four times that of natural gas per MWh. However, this cost is anticipated to decrease by half by the year 2040 (Vattenfall AB [2024]). Keep in mind that these prices are subject to change by 2040, and carbon prices are not factored in. The model will incorporate Vattenfall's forecasts as initial inputs, with subsequent sensitivity analyses exploring the impact of fuel price variations.

3.3.4 Heat demand

3.3.5 Supply and return Temperatures

The supply and return temperatures of a district heating network are two key operational parameters. The optimization of supply temperature control is a key focus in third-generation district heating networks, where maintaining a high delta between supply and return temperatures is crucial for maximizing distribution capacity. Equation 3.4 describes the total power delivered to consumers in equivalent heat. In fourth-generation district heating networks, the emphasis shifts towards reducing the supply temperature. This allows for the integration of low-temperature renewable heat sources, offering advantages such as decreased heat loss and improved Coefficients of Performance (COPs) for heat pumps. However, lowering the supply temperature comes with trade-offs. While it reduces heat loss and enhances COPs for heat pumps, it also decreases transport capacity (refer to equation 3.4).

As previously discussed, the supply temperature plays a significant role in adjusting heat load demand, therefore literature has been focused on forecasting heat demand and implying control strategies for supply temperature accordingly. Given that consumers are situated at different distances from the heat source, there exists a delay in heat supply, which needs to be factored into supply temperature control strategies. This delay is affected by the flow velocity, usually around 1 *m/s* (Chertkov and Novitsky [2019]). The flow velocity is kept around this benchmark for practical and economical reasons.

$$\phi_c = \dot{m}_c c_p (T_s - T_r) \tag{3.4}$$

$$\phi_c(t) \approx \dot{m}_c c_p (T_s(t - \tau_s) - T_r(t + \tau_r)) \tag{3.5}$$

The consumer heat load (ϕ_c) is expressed in Equation 3.4, where the mass flow rate ($\dot{m}_c$) is influenced by pumping control strategies. By controlling pumps, a desired mass flow and pressure difference can be achieved. The primary optimization goal is to minimize pumping costs. T_s and T_r denote the supply and return temperatures, respectively, with the supply temperature often controlled by a mechanism correlated with outdoor temperature. Stochastic black and grey box models are employed to determine return temperatures, as discussed in the literature Laakkonen et al. [2017].

To account for delays in the system, Equation 3.5 is introduced. The delayed consumer heat load ($\phi_c(t)$) is approximated by considering delayed temperatures ($T_s(t - \tau_s)$ and $T_r(t + \tau_r)$), where τ_s represents the delay from supplier to consumer, and τ_r is the delay back from consumer to supplier. Notably, the delay factor is time-dependent, varying with mass flow. Zheng et al. [2022] derived a numerical model which describes the return temperatures and delay time, this model was validated by a DHN in Changchun. The delay time was ranges between 21-24 *min/km*.

3.3.6 Mass flow control

A district heating network can be effectively modeled using the methodology of two balances: the thermal and hydraulic balance. While this section focuses on the latter. Hydraulic models will be out of the scope of this simplistic study, never the less a broader understanding of how the mass flow is controlled is desirable. The mass flow is predominantly regulated by establishing a pressure difference in the DHN, with the primary pressure losses arising from turbulence and friction.

$$\sum_{in} G_{in} - \sum_{out} G_{out} - \sum_{u} G_u = 0 \tag{3.6}$$

$$\Delta p_{ij} - (p_i - p_j) = 0 \tag{3.7}$$

The hydraulic model is built upon two fundamental conservation laws. Firstly, mass conservation is considered (equation 3.6). These equations are structured to represent the entire system through nodes, where each node conservation of mass should apply. Here, G_{in} represents the volumetric flow in m^3/s entering the node, G_{out} describes the volumetric flow leaving the node, and G_{u} represents the flow towards the user. Secondly, a pressure balance is maintained between each pair of nodes, as expressed in equation 3.7. In this equation, Δp_{ij} denotes the pressure loss between nodes i and j, while p_{i} and p_{j} are the inlet and outlet pressures, respectively, measured in Pa.

In piping systems such as district heating networks, two main types of hydraulic losses prevail: frictional losses resulting from the flow of the medium (water) along the pipe's surface, and minor losses arising from changes in streamline through valves, bends, and other components. Equation 3.8 provides an expression for the pressure drop, considering the non-linearity that must be addressed when employing a linear modeling approach.

$$\Delta p_{ij} = \frac{8\rho}{\pi^2}\left(\frac{\lambda_{ij} L_{ij}}{D_{ij}} + \zeta_{ij}\right)\frac{G_{ij}^2}{D_{ij}^4} \tag{3.8}$$

In this equation, ρ denotes the density of water in kg/m^3, L_{ij} is the pipe length in meters, D_{ij} represents the inner diameter of the pipe segment in meters, and G_{ij} is the volumetric flow in m^3/s. The Darcy-Weisbach friction factor (λ_{ij}) depends on the Reynolds number, relative roughness, and kinematic viscosity. Finally, the term ζ_{ij} accounts for minor losses in the system.

3.3.7 CO2 emission per asset

One of the sub-questions is ”how to minimize the carbon footprint of the delivered heat.” To address this, an understanding of the carbon footprint per heat source must be determined. ”de Warmtewet” is a Dutch law outlining how heat producers should register their emissions for delivered heat, this study will only focus on CO_2 emissions. Emissions vary based on the heat source, fuel type, and the timing of electricity usage. A summation of all the assets is provided below, and additional details can be found in the methodology or in the reference Harmelink:

- **CHP**
  In a CHP system, electricity production is sacrificed to extract heat from the steam cycle. The electricity sacrificed in this process is assumed to be produced in another natural gas-fired power plant, the carbon footprint of this electricity production will be assigned to the heat deliverd.
- **E-Boiler and Heat Pumps**
  There are two ways of dispatching the E-boiler in this registration domain. First, it can be dispatched when electricity prices are below a certain benchmark. Heat production does not follow the heat demand but overproduces in combination with a storage capacity. This benchmark price is the marginal cost for fossil-based electricity production and is determined daily (known as the DRP). When the electricity price is below this benchmark, it is assumed that the heat is produced with renewable electricity, resulting in a zero carbon footprint. When operating above this point, the electricity will have the nationwide averaged carbon intensity divided by the COP of the asset.
- **Geothermal**
  The heat gained from the geothermal source is considered renewable. Only the auxiliary (heat) pumps's electricity usage will be measured similarly to a normal heat pump.
- **Peak Boilers**
  Peak boilers will be measured with regard to their fuel usages, assuming an efficiency of 99 %.

3.4 Numerical modeling

The study aims to determine the optimal capacity for integrated heat storage in the scenario outlined in Chapter 1. District heating network modeling involves two primary components: hydraulic and thermodynamic models, which cover pumping characteristics, pressure loss, mass flow, operating temperatures, and supplied heat; and control mechanism models that focus on asset dispatch based on heat demand and electricity prices. While this study primarily focuses on optimizing assets in conjunction with storage capacity, a brief overview of other modeling aspects and methods is provided in section 3.4.1. In this chapter, a modeling approach for the Thermal Energy Storage (TES) is also introduced, aiming to determine both the heat loss to the environment and the degradation of temperature on an exergy level. Further examples of methods on operating strategies are given in paragraph 3.4.2. To finish with different optimization methods are proposed

3.4.1 Review on modeling

In literature, two main types of models are used: deterministic and stochastic. Deterministic models provide consistent output with the same input, ensuring robustness but possibly oversimplifying the problem. Stochastic energy models, like regression models and artificial neural networks, handle uncertainty and variations in input parameters. The choice of modeling software depends on the desired level of detail.

Contrasting to deterministic approaches, regression models offer a solid mathematical foundation, displaying straightforward implementation due to well-studied behavior. However, their accuracy diminishes in the absence of clear input-output correlations. Artificial Neural Networks (ANNs) are effective in handling numerous parameters, displaying self-learning behavior and reliability in output data quality. Probabilistic models, such as those used in forecasting end-user heat demand and electricity pricing, become relevant when uncertainty is present, as exemplified by Aydinalp-Koksal and Ugursal [2007], who derived a model describing the relationship between weather forecasts and end-user energy consumption using neural networks.

Existing literature, like Gu et al., extensively explores optimizing Combined Heat and Power (CHP) control, providing insights into modeling, planning, and optimal energy management. Understanding the thermal-hydraulic aspects of the distribution network is crucial, outlined in Sarbu et al. [2019] for hydraulic and thermal losses. Significant contributions also come from forecasting models for end-user heat demand, discussed in Olsthoorn et al. [2016].

Furthermore, KRZYSZTOF BADYDA [2014] presents a comprehensive model of a back-pressure extraction turbine, validated with operational data. Although complex, it serves as a reference model for simpler alternatives. Another empirical model by Szapajko and Rusinowski [2010] emphasizes simplicity and quick calculations, acting as a bridge between thermodynamics and computer modeling. Additionally, Le Sko et al. [2018] incorporates a thermal storage system interacting with a CHP plant. Shifting focus to the district heating network, recent years have witnessed the development of numerous thermo-hydraulic models, exemplified in Oppelt et al. [2016] and Brange et al. [2017]. To construct a realistic model, it is essential to thoroughly study key parameters.

3.4.2 Determenistic controlling strategy

In a deterministic modeling approach, assets are controlled based on input variables like heat demand, electricity price, and carbon intensity. The key characteristic is that given the same input, the output remains constant. Typically, the approach involves a simplified representation of a District Heating Network (DHN), incorporating different assets, heat flows, and standardized loss factors to model real physical properties. For example, in Siddiqui et al. [2021], optimal thermal energy storage in combination with a heat pump is studied using an idealized stratified water tank.

Figure 3.8 illustrates a deterministic decision-making flowchart. Input variables, including the bottom temperature of the storage tank, guide the system. The bottom temperature serves as an indicator of the state of charge in the storage tank, as explained in 3.2. The system comprises multiple Combined Heat and Power (CHP) units and peak boilers. When electricity prices are high but there is no proportional heat demand, CHP units are dispatched, and excess heat is stored. Conversely, when electricity prices are low, the CHP plant is not run to meet heat demand, and the storage is utilized.

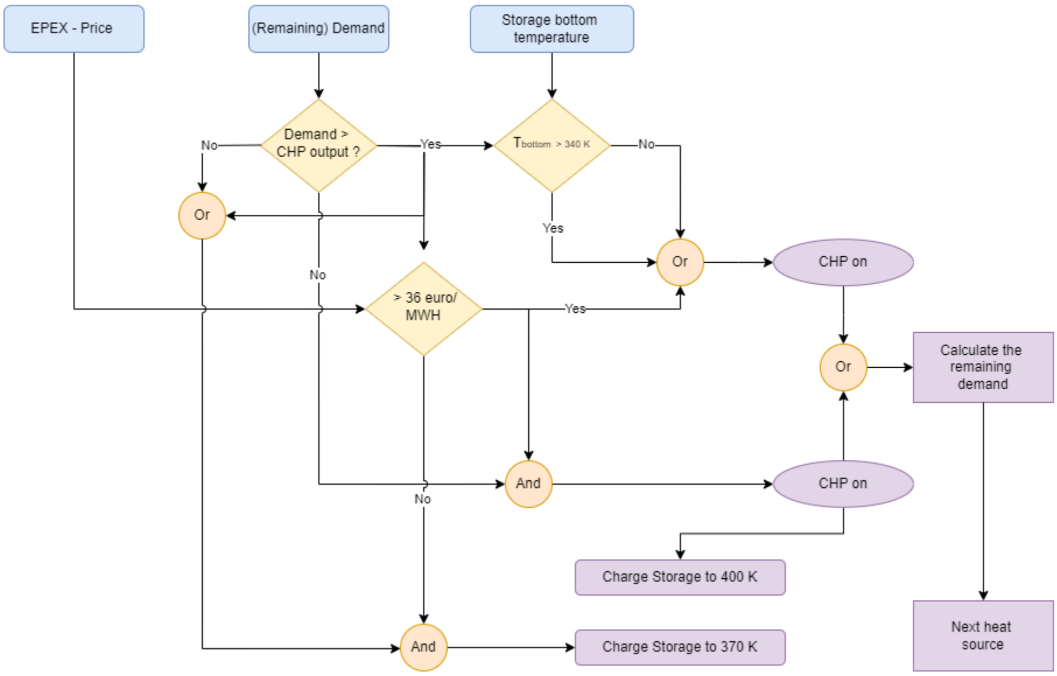

Figure 3.8: Charging TES flowchart

Modelica/DYMOLA is a commercially available software program used for modeling energy systems, employing mathematical equations aligned with the physical modeling paradigm. Additionally, it provides a graphical interface for model setup and input variables. Dahash et al. [2019] used Modelica to design a mathematical control strategy for a Combined Heat and Power (CHP) system combined with thermal storage, using European Energy Exchange (EEX) prices as input for an optimal operating strategy. The foundational control scheme is based on an earlier study by Dahash et al. [2017], outlining the control strategy for a CHP plant in conjunction with a district heating network. The model demonstrates a root mean square error of $\leq 7\%$, considered a ”good” approximation of reality.

The study evaluates various Thermal Energy Storage (TES) volumes, revealing a reduction in peak boiler dependency with an increasing storage volume. Implementing pricing data from 2020 results in a 3% net profit increase with a storage capacity of 1200 m^3. Note that the model is not designed to handle negative prices, and it is recommended to run boilers instead when EEX prices turn negative (Dahash et al. [2019]).

3.4.3 Optimization

In deterministic modeling, a key step is optimization, answering questions like finding the storage capacity that minimizes heat pricing or carbon intensity. Linear programming is a common method for optimization in engineering, involving a system of linear equations with constraints. Defining an objective function allows optimization of outcomes like production cost. Note that non-linear aspects may require linear approximations, a limitation of the Mixed-Integer Linear Programming (MILP) method. For power production planning, Viana and Pedroso [2012] outlines an MILP-based approach. It provides a stepwise guide for setting up the MILP, covering system constraints, technical constraints, and computational variable establishment.

Linear programming is mainly used for planning in Combined Heat and Power (CHP) plants, spanning time frames from a few hours (day-ahead) to several years. Lahdelma and Hakonen [2003] developed an algorithm optimizing the controls of a system involving heat and power. To grasp linear programming basics, the governing equations discussed in equation 3.9 form the foundation for various linear programming approaches, including Mixed-Integer Linear Programming (MILP).

The algorithm's aim is to minimize energy production and purchase costs. Here, $\mathrm{z(x)}$ is the optimization function, with $\tilde{\mathrm{x}}$ as a vector of decision variables. The energy system is divided into independent subsystems $u \in U$, representing different heat sources, each with its net cost function $\mathrm{C_u(x_u)}$. These subsystems describe each hour of the energy balance in $t\ inT$, with the balance shown as the transmission matrix H, where b^t corresponds to the demand forecast. Subsystem-specific constraints are represented by sets X_u. Model constraints ensure the heat demand is always met. The next step combines the energy balances and the objective function. When combined, the linear objective function $z(x)$ is minimized, providing an optimal decision variable x. In this case, the SIMPLEX solver is used. Wang et al. [2015] extends the approach from Lahdelma and Hakonen [2003], including heat and electrical storage. In Python, a widely-used linear programming module is Pyomo. This module allows you to define a set of variables and an objective function, which can then be optimized using a linear solver. In the context of this paper, Gurobi is proposed as solver. Gurobi is a commercially available solver licensed by Vattenfall, making it the logical choice to use.

$$min\ z(x) = \sum_{u \in U} C_u(x_u) \tag{3.9}$$

$$s.t.\ H\vec{x}^t = \vec{b}^t \quad ,t \in T \tag{3.10}$$

$$x_u \in X_u \quad ,u \in U \tag{3.11}$$

Instead of using linear programming, Siddiqui et al. [2021] purposes a dynamic optimization algorithm to optimize Thermal Energy Storage (TES) capacity over a 5-day period. This approach is adapted from an open-source Python library called Prodyn. The paper explains how a deterministic model can be discredited in detail.

3.5 Conclusion

The literature review aimed to understand both the physical and modeling aspects of district heating, including pricing dynamics. In Section 3.1, the focus shifted to electricity and the power-to-heat market, covering marginal costs and defining key model input parameters. The first step in creating an optimal control strategy, the merit-order, was introduced. Section 3.2 discussed various thermal storage techniques, highlighting the preference for sensible heat storage due to its maturity and alignment with the district heating network's temperature range. Moving to Section 3.3, the thermodynamic behavior of assets and the district heating network was explored, emphasizing the modeling of supply and return temperatures and incorporating distribution delay. Lastly, Section 3.4 discussed numerical modeling methods, reviewing literature on techniques and proposing linear programming as the optimization method. On the other hand, the finite difference method is proposed for deriving a thermodynamic model. With this understanding.

Now a fundamental understanding of the district heating environment is stated the first hypothesis to answer the research question's can be proposed. To start with the time span, from literature and electricity pricing evaluation

3.5.1 Hypothesis

The research aims to quantify the impact of thermal energy storage (TES) on the carbon footprint and cost of delivered heat in a fourth-generation district heating network between 2030 and 2040. This impact is influenced by various input variables, including changes in heat asset configuration, electricity pricing dynamics, fuel prices, and carbon emission prices. To quantify this impact a numerical optimalization model is developed. To address the correlation between these variables and the model output, hypotheses are formulated to answer specific related questions.

Question I: How will larger storage capacities correlate with the model outcome?

Hypothesis I: The implementation of larger thermal storage capacity will result in increasing reduction of heating costs, following a logarithmic correlation pattern that eventually converges to an asymptote.

Rationale I: Initially, an increase in storage capacity will yield significant gains by leveraging daily fluctuations in heat pricing. However, as storage capacity continues to grow, diminishing returns may be observed, particularly as seasonal differences in heat pricing become more influential. As the storage time increases, the gain per MWh of storage capacity is anticipated to decrease. The asymptote represents the maximum gain achievable with available overcapacity during favorable hours.

Question II: How will financial gains change over the modeling time span?

Hypothesis II: Financial gains are anticipated to decline over the modeling period.

Rationale II: This decline in financial gains can be attributed to various factors, including changing electricity prices, reduced operational costs of assets, and rising prices of fuels and carbon emissions. Asset configuration is important too, as there needs to be extra capacity to charge the buffer at lower prices.

Question III: How will carbon intensity change over the modeling time span?

Hypothesis III: The effectiveness of storage capacity in reducing the carbon footprint will decrease over time.

Rationale III: Changes in asset configurations, such as the retrofitting of combined heat and power (CHP) systems to hydrogen-fired systems, along with the decreasing carbon intensity of electricity grids, will contribute to lowering the overall carbon footprint of the district heating network. Consequently, the effectiveness of TES in further reducing carbon intensity is expected to diminish over time.

4 Method

Having established a fundamental understanding of the existing research on this topic, a roadmap for addressing the research questions effectively is essential. The goal is to assess the impact of thermal energy storage on financial and environmental performance. Achieving this requires a numerical model with a fast computational time, enabling the analysis of multiple storage capacities and their impact on the research objectives.

A numerical model of the district heating network of Amsterdam-East/Almere has been developed. With a given asset configuration and heat load, the heat load is modeled as a sink and heat sources as a source, without implementing hydraulic constraints. Additionally, a finite difference model of the heat storage quantifies heat diffusion and losses over a mid-short modulation interval.

The model will analyze numerical results and express them in benchmark metrics, quantifying the economic and environmental value of the implemented thermal energy storage.

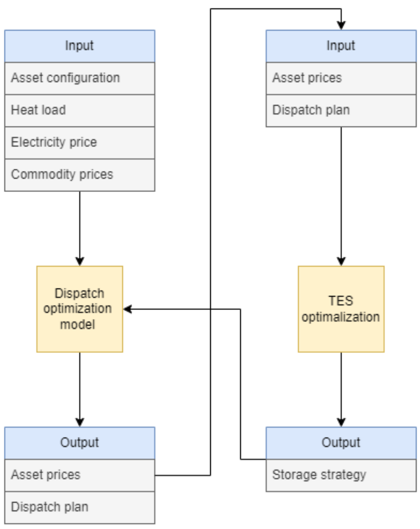

Figure 4.1: Numerical model flowchart

The model consists of two sub-optimization problems, as illustrated in Figure 4.1. The first sub-optimization involves the Dispatch Optimization Model, which optimizes asset dispatch to meet heat demand using various input variables to generate an initial dispatch plan. The second sub-optimization determines the charging and discharging strategy of the thermal storage capacity using time series data. This process is complex and requires machine learning methods such as linear programming. The resulting storage strategy is then fed back into the Dispatch Optimization Model. In this second optimization step, the final dispatch plan is produced, incorporating the optimized storage strategy.

Lastly the model has two primary objectives: to minimize the cost of delivered heat and to minimize the carbon footprint of the delivered heat. Both objectives are combined in a hybrid version of the model to achieve an optimal balance. The optimization is subjected to several constrains, listed below:

Constrains:

- Heat Demand Constraint
- Maximal Storage Capacity Constraints
- Operational Constrains
- Economic Constrains
- Environmental Constraints

Additionally, the model includes a thermodynamic model to visualize and analyze exergy and heat loss constraints, as an example the evolution of heat diffusion within the storage capacity. A one-dimensional finite element method is chosen for the thermodynamic model, which will be implemented using the charging and discharging strategy obtained from the previous optimization step.

4.1 Input variables

The model relies on specific input data to simulate the operation of the heat storage capacity over a year. This data, provided as a perfect forecast, includes various variables for the years 2023, 2030, 2035, and 2040. Specifically, in 2040, the transition from natural gas to hydrogen fuel is expected. The heat load is forecasted at the Diemen production site, where all assets are centralized, removing any transportation delays.

Commodity prices are forecasted using LTMO (Long-Term Market Outlook), an econometric model offering hourly forecasts. This model is based on historical data and expected market trends, incorporating an increasing share of renewable energies like wind and solar, as well as flexible power demand. Secondly the heat demand is an indexed at the year 2022, a heat load reduction of 3 % is taken into account due to insulation measurements. For the heat load, a gradually expansion is forecasted. The initial year of 2023 serves as a reference point for the analysis. Further statistical evaluation of these forecasts is discussed in Chapter 5.

Table 4.1: Model input data

Data	Unit	Resolution
Electricity prices	*€/MWh*	Hourly
Heat load	*MW*	Hourly
Carbon price	*€/t*	Monthly
Gas price	*€/MWh*	Monthly
Hydrogen price	*€/MWh*	Monthly

Due to confidentiality constraints, the input variables of the model are not publicly disclosed. Therefore, a description is provided. For electricity pricing, it is observed that during the modeling period, the prices stabilize around lower electricity prices. The higher price regime becomes more extreme, with prolonged periods of high prices, primarily during times when renewable energy availability is low. A distinctive difference in prices between winter and summer is noted, with more less expensive hours occurring in summer. These phenomena are expected to alternate in time.

Regarding commodity prices, the gas prices for 2030 and 2035 are relatively affordable, while hydrogen prices in 2040 are significantly higher. However, the increasing costs associated with carbon footprint bonds largely balance out this difference. Naturally, the heat load is lower in summer compared to winter. In summer, the heat load is around 100 *MW*, whereas in winter, the average heat load is approximately 450 *MW*.

4.2 Heat assets

In this section, the numerical modeling of all the included heating assets is discussed, along with a fundamental description of the correlation between electricity prices, heat prices, and the carbon footprint. Table 4.2 presents the asset configuration within the modeling domain. First, the thermal power of the CHPs is divided between two plants, namely Diemen 33 and 34. It can be seen that in the year 2040, Diemen 33 will be decommissioned, and Diemen 34 will be retrofitted to a hydrogen-fired CHP. In paragraph 4.2.1, the modeling of the CHP is further elaborated on, detailing the characteristics of both assets. It can be observed that the reference year of 2023 heavily relies on the dispatch of CHP, especially given the prediction of lower electricity prices. "Must runs" become inevitable when the asset configuration is not diversified. Coinciding with the desire to lower the carbon footprint of the district heating network, significant changes are made to the source strategy starting in the year 2023. A graphical representation of the model including all the asset streams is given in 4.2.

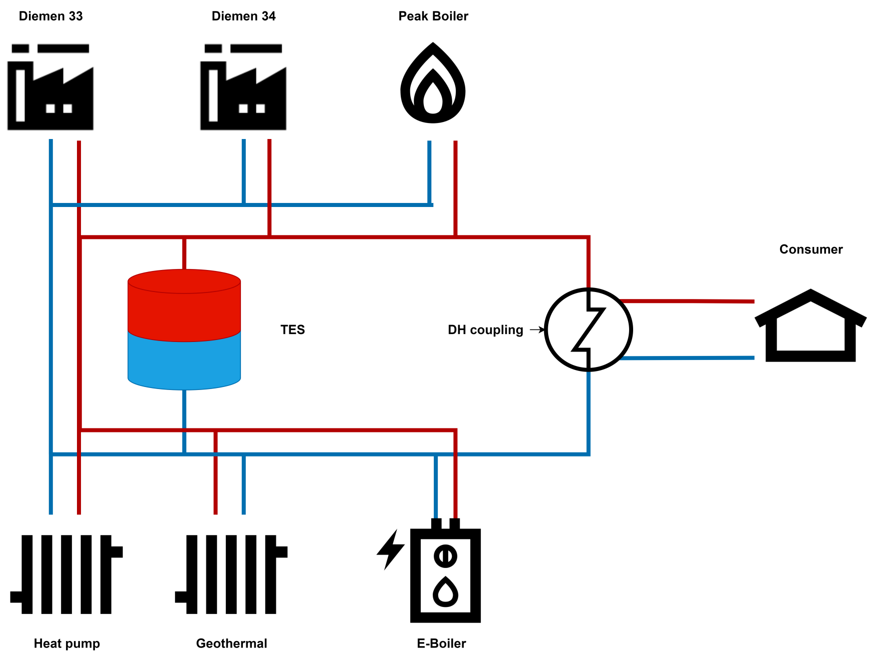

Figure 4.2: Model visualisation

Table 4.2: Projected Thermal Power (*MW*) per Source Type

Year	CHP (CH_4 /H_2) (*MW*)	E-boiler (*MW*)	Heat Pump (*MW*)	Geo-thermal (*MW*)	Boiler (CH_4 /H_2) (*MW*)
2023	440	–	–	–	650
2030	440	150	31	30	650
2035	440	150	41	80	730
2040	260	150	101	100	800

For the E-boiler, Heat Pump, and the geothermal heat source, the calculation is straightforward, as indicated by Formula 4.1. Here, the grid fees and subsidies are OPEX-related and provided per *MWh* of produced heat. Equation 4.2 provides the unit price of heat produced by the boiler (in EUR/MWh), considering both the fuel price and the carbon price. The latter is multiplied by the Emission Factor (EMF).

$$\text{Price}_{\text{EB/HP/GEO}} = \frac{\text{Price}_{\text{elec.}} + \text{Grid}_{\text{Fee}} + \text{subsidies}}{\text{COP}} \tag{4.1}$$

$$\text{Price}_{\text{BO}} = \frac{(\text{Fuel}_{\text{Price}} + \text{Carbon}_{\text{Price}}) * \text{EMF}}{\text{COP}} \tag{4.2}$$

4.2.1 Combined Heat & Power plant

It can be said that the CHP asset is one of the more complex heat producing assets. Partly because, the asset is active on both the power and the heat market. Electricity has to be produced to generate heat, creating a certain dependency on the electricity market. Another aspect is the differing plant efficiency, which varies between load levels. While the load has to be known as an input for the producing costs, an additional optimization step has to be made.

To understand how the CHP will be modeled, the PQ diagram (see 4.3) will shortly be reintroduced. On the vertical axis, the electric load is displayed. When no heat is needed, it will operate here, also referred to as full condensing mode (line **A-D**), here only electricity is produced. Secondly, we have line **A-B**, where the heat production is maximal as is the electricity production. When electricity prices are above the marginal cost of producing electricity, the model will choose to operate on this line (maximal fuel line), while producing maximal electricity to the grid. The electricity production is sacrificed with a ratio of 1 to 5, this means that for every *MW* of sacrificed electricity production 5 *MW* of heat is created. When heat is needed but electricity prices are unfavorable, for instance when they are below the marginal cost, the model will descend to line **D-C** (minimal fuel line). It is crucial to understand that when the plant is operating when electricity prices are below the marginal costs (must-run), the losses are spread over the heat production. So in this case operating further up the Q line is more favourable. When maximal heat is needed, it will descend line **B-C**, also known as the maximal heat line.

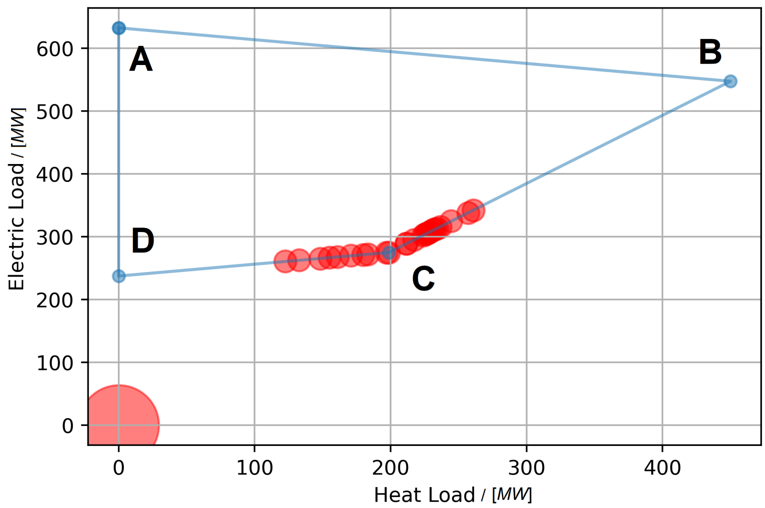

Figure 4.3: CHP PQ-Diagram

In Figure 4.3, an example is provided of how the CHP is dispatched. This demonstration is based on an autumn day characterized by relatively low electricity prices and a moderate heat demand. The marginal cost of producing electricity is larger than the price of electricity. Consequently, the plant primarily alternates between the minimal fuel and maximal heat lines. This is to minimize losses incurred on the electricity market, a practice known as "must run," to meet the heat load.

In the district heating network of Amsterdam, two separate CHP units are integrated: the Diemen 33 and the Diemen 34. Additionally, Diemen 33 is scheduled for decommissioning after the year 2035. Furthermore, Diemen 34 is scheduled for retrofitting into a hydrogen-fired CHP post-2035. This model will individually simulate both assets, and the specifications outlined in Table **??** are assumed to remain constant throughout the modeling period. ($\eta_{\text{elec.}}$) represents the efficiency of producing electricity, this ranges between 34 % to 59%, which is load depending. Also the power loss ratio (PL_{ratio}) differ between both production facilities. The power loss factor is in a range of 0.15 to 0.20 $\frac{MW_{\text{elec.}}}{MW_{\text{heat}}}$

The price of produced heat is heavily dependant on where the CHP is operating in its PQ-diagram and the price of electricity. The price of producing electricity will be recalled to as the marginal costs (see equation 4.3) , these differ in the PQ-diagram, mainly depending on $\eta_{\text{elec.}}$. Also the price of the fuel and cost of carbon emission rights are taken into account,this is the multiplication of $\dot{\text{F}}$ times the fuel cost and carbon emission price . Where $\dot{\text{F}}$ represents the fuel flow in $\frac{kg}{h}$.

$$\begin{aligned}
&\text{Price}_{\text{marg.}} = f(P, Q, \text{Fuel}_{\text{price}}, \text{Carbon}_{\text{price}}) \\
&\text{Price}_{\text{marg.}} = \dot{F}(\text{Fuel}_{\text{price}} + \text{Carbon}_{\text{price}}) \\
&\quad \text{where:} \\
&\qquad \dot{F} = \frac{P}{\eta(P, Q)}
\end{aligned} \tag{4.3}$$

Now that the marginal cost of operating the CHP is defined in the PQ-diagram, the derivation of the cost of produced heat can be made. To do this, two operating states are introduced: "in the money" and "out of the money". When being "in the money", means that the plant is making money on the electricity market ($\text{Price}_{\text{elec.}} > \text{Price}_{\text{marg.}}$). In this case, the price of heat is derived as the electricity price multiplied by the PL_{ratio}. Where the PL_{ratio} is the ratio of electricity production sacrificed to produce heat, this should be multiplied with the price of electricity. With the rhetoric that the sacrificed electricity would else wise have been sold to the grid. It's important to note that the CHP will be dispatched at the maximal fuel line (A-B) while maximizing electricity production is favourable when the plant is "in the money".

$$\begin{aligned}
&\text{Price}_{\text{CHP}} = f(P, Q, \text{Fuel}_{\text{price}}, \text{Carbon}_{\text{price}}) \\
&\text{when "in the money" } (\text{Price}_{\text{elec.}} > \text{Price}_{\text{marg.}}): \\
&\text{Price}_{\text{CHP}} = \text{Price}_{\text{elec.}} \cdot PL_{\text{ratio}}
\end{aligned} \tag{4.4}$$

Now let's discuss the scenario where the electricity price is lower than the marginal cost ("out of the money"). Ideally, one would stop electricity production, which means shutting down the plant entirely. However, if heat is still needed, the losses of electricity production ($(\text{Price}_{\text{elec.}} < \text{Price}_{\text{marg.}}) \cdot \text{P}$) have to be divided by the heat production. This means that when operating ”out of the money”, production of heat should be maximized to spread this loss over a greater amount of heat.

$$\begin{aligned}&\text{When ”out of the money” } (\text{Price}_{\text{elec.}} < \text{Price}_{\text{marg.}})\text{:}\\ &\text{Price}_{\text{CHP}} = \frac{(\text{Price}_{\text{elec.}} - \text{Price}_{\text{marg.}}) \cdot P}{Q}\end{aligned} \tag{4.5}$$

The model incorporates the following constraints and assumptions:

Constraint I: ”When the plant is making money on the electricity market, it will be operated at line **A-B**”.

Constraint II: ”If the CHP is partly ”in the money” due to efficiency differences, it will be operated at maximal efficiency”.

Assumption I: ”The efficiency at lines **A-B**, **B-C**, and **C-D** are taken to be constant”.

Assumption II: ”No delays in heat extraction are considered in the calculations”.

Assumption III: ”The dispatch strategy does not account for the participation of the CHP in grid balancing”.

Constraints I & II are implemented to maximize the plant revenue on the electricity market. Furthermore, it can be seen that by these constraints, the price of heat is only dependent on the power loss ratio (PL_{ratio}) at line **A-B**. The response time of the CHP is primarily influenced by power production, and since power production is not optimized and there is no delay in heat extraction, Assumption II is considered valid. Additionally, the role of the CHP as a balancing service provider is neglected, as imbalances are primarily random and challenging to model. Therefore, imbalance dispatch is not considered a significant source of uncertainty in this study. Further code snippets are provided in Appendix A (see Section 9).

4.2.2 Start-up costs

While CHP units possess significant thermal inertia, starting them up incurs considerable costs primarily due to additional maintenance and startup inefficiencies. Therefore, it is crucial to account for startup costs as a constraint. These costs become especially significant when CHP units shift from their base-load role. When operating "out of the money," the CHP units will be shut down, making the startup costs more impactful. In the numerical model, the startup cost of the CHP is set as a constraint, with slack variables used to determine if a hot, cold, or warm start is applicable. The startup costs used are displayed in Figure 4.3.

Table 4.3: Flexibility parameters natural gas combined cycle (Brouwer et al. [2015])

Ramp rate (%/min)	Start-up time (h)			Start-up cost (€/$MW_{installed}$)		
	Hot start	Warm Start	Cold start	Hot start	Warm Start	Cold start
6 ± 2	$1 \pm \frac{1}{2}$	$2 \pm \frac{1}{2}$	3 ± 1	27 ± 11	39 ± 20	57 ± 29

4.3 Linear Programming optimization

First, let's start with the hourly heat assets dispatchment, which can be hardcoded as a fully defined problem, but this is not the most computationally efficient way. Therefore, this is also optimized using linear programming. Linear programming is an optimization technique, so let's provide a brief introduction to the concept.

Linear programming (LP) is a mathematical optimization technique used to maximize or minimize a linear objective function subject to a set of linear equality and inequality constraints. The objective function represents the quantity to be maximized or minimized, while the constraints represent the limitations or restrictions on the decision variables.

In Linear Programming (LP), decision variables are used to represent the quantities to be determined, and these variables are typically subject to certain constraints. The goal of linear programming is to find the values of these decision variables that optimize the objective function while satisfying all constraints.

LP problems are characterized by the following components:

1. Objective function: A linear function representing the quantity to be optimized.
2. Decision variables: Variables representing the quantities to be determined.
3. Parameters are fixed values provided as input to the LP model, remaining constant throughout the optimization process.
4. Constraints: Linear inequalities or equations that impose limitations on the decision variables.

The solution to a linear programming problem involves finding the values of the decision variables that maximize or minimize the objective function while satisfying all constraints. This is typically achieved using optimization algorithms such as the simplex method or interior-point methods.

For the heat asset dispatchment control, there are two ways to control the assets: first by minimizing the cost of produced heat and secondly by minimizing the carbon footprint. To do so, the Pyomo package is used, which is a language to define LP problems. As an example, the objective function for heat dispatchment is shown in Listing 9.1, and all objective functions and constraints are added in Appendix A (9). In the objective function, the parameters are the price of produced heat per asset at that timestamp. This is multiplied by the variable which describes the assets dispatchment. This should be minimized for all timestamps, while no storage is included, and every timestamp is independent from each other. Constrains here were mainly the asset maximal capacity and the heat-load.

Objective function dispatch model

$$Z = \sum_{t \in T} (\mathrm{Load}_{\mathrm{CHP}}[t] \cdot \mathrm{Price}_{\mathrm{CHP}}[t] + \mathrm{Load}_{\mathrm{HP}}[t] \cdot \mathrm{Price}_{\mathrm{HP}}[t] + \mathrm{Load}_{\mathrm{EB}}[t] \cdot \mathrm{Price}_{\mathrm{EB}}[t] \ \ \text{etc...}) \tag{4.6}$$

In 4.2.1 the dependency of the price of heat regarding to the operating points in the PQ-diagram was introduced. Therefore the price and load of the CHP are not known. This means that when $\text{Price}_{\text{CHP}}[t]$ is multiplied with $\text{Load}_{\text{CHP}}[t]$ a bi-linear equation occurs (involving a multiplication of two variables, like $z = x \cdot y$). Linear programming can handle bilinear objective functions to a certain extent, but it does not allow for a convex solving method in this case. Convex solvers are desirable because they ensure that any local optimum is also a global optimum, and they can typically be solved efficiently. Since the model aims to be computationally efficient and find a global optimum, this problem needs to be addressed further.

Another issue arises when describing the relationship between the CHP load and its price. As shown in Equations 4.5 and 4.7, the marginal costs depend on the load ($\text{Load}_{\text{CHP}}[t]$) and the power production ($P[t]$), and the price function includes a division by the decision variable $\text{Load}_{\text{CHP}}[t]$. This makes the constraint nonlinear, posing another challenge when solving the problem with linear methods. A linear solving strategy is preferred for its ability to handle large datasets effectively.

Price constraint CHP

$$\text{Price}_{\text{CHP}}[t] = \frac{(\text{Price}_{\text{elec}}[t] - \text{Price}_{\text{marg}}[t]) \cdot P[t]}{\text{Load}_{\text{CHP}}[t]} \tag{4.7}$$

To avoid a bi-linear objective function and the nonlinear price constraint, a binary variable $\tilde{y}[t]$ is introduced. Binary variables can only take values of 0 or 1, effectively eliminating the bi-linearity in the objective function. The binary variable $\tilde{y}[t]$ is multiplied by a finite set of n price points, corresponding to pre-defined load points. Equation 4.8 demonstrates how a set of pre-defined load points from the PQ-diagram are substituted into Equation 4.7. This results in an array containing the corresponding price points.

$$\begin{aligned}
y[t] &= \begin{bmatrix} y_1 \\ y_2 \\ \vdots \\ y_{n-1} \\ y_n \end{bmatrix} \qquad P = \begin{bmatrix} 0 \\ 160 \\ \vdots \\ 410 \\ 420 \end{bmatrix} \\
Q &= \begin{bmatrix} 0 \\ 10 \\ \vdots \\ 250 \\ 260 \end{bmatrix} \qquad \text{Price}_{\text{points}}[t] = \begin{bmatrix} \text{Price}(P[1], Q[1], \text{Price}_{\text{elec}}[t]) \\ \text{Price}(P[2], Q[2], \text{Price}_{\text{elec}}[t]) \\ \vdots \\ \text{Price}(P[n-1], Q[n-1], \text{Price}_{\text{elec}}[t]) \\ \text{Price}(P[n], Q[n], \text{Price}_{\text{elec}}[t]) \end{bmatrix}
\end{aligned} \tag{4.8}$$

To ensure that the solver selects only one load point, a "Binary constraint" is introduced as shown in Equation 4.10. The updated objective function is given by Equation 4.9. In this formulation, the solver evaluates all prices and corresponding loads and optimizes the decision variable $y[t]$. It's important to note that $\text{Price}_{\text{points}}$ and Q_n are parameters that remain constant at each timestep. This adjustment allows for the optimization of CHP dispatch and allows for a linear convex solving method.

Adjusted objective function

$$Z = \text{Price}_{\text{points}}[t][n] \cdot Q[n] \cdot y[t][n] + \text{Load}_{\text{HP}}[t] \cdot \text{Price}_{\text{HP}}[t] \ \text{ etc..)} \tag{4.9}$$

Binary constrain

$$\sum_{i=1}^{n} y_i[t] == 1 \tag{4.10}$$

The (dis)-chargin strategy is more colmplex, involving inter dependencies among 8700 timesteps. In Listing 9.2, the second objective function is presented. It incorporates real-time asset prices as parameters ($\mathrm{Price}_{\mathrm{CHP}}$ etc..). These parameters are multiplied by the variables representing the charging loads. Additionally, the discharging variable ($\mathrm{TES}_{\mathrm{discharge}}$) is included, multiplied by the price of heat when no storage is implemented. The function is optimized by exploring all possible dispatchments. This objective function ensures that the Thermal Energy Storage (TES) system is discharged during periods when the cost of heat is high, thereby maximizing cost savings and efficiency. This function is maximized using linear programming. Furthermore, several constraints are defined for the optimization process, such as the maximal storage capacity, detailed in Listing 9.3. This constraint describes the state of charge SOC[T], ensuring that the maximum storage capacity is never exceeded when optimizing the objective function. The same steps are also undertaken for the minimization of the carbon footprint.

Objective function TES model

$$Z = \sum_{t \in T} \Big(TES_{discharge}[t] \cdot Price_{without-storage}[t] - Charge_{\mathrm{CHP}}[t] \cdot Price_{\mathrm{CHP}}[t] \;\; \text{etc...} \Big) \tag{4.11}$$

Constraint for Storage Balance

$$\mathrm{SOC}[t] = \mathrm{SOC}[t-1] - \mathrm{TES}_{\mathrm{discharge}}[t] + \mathrm{Charge}_{\mathrm{CHP}}[t] + \mathrm{Charge}_{\mathrm{EB}}[t] + \mathrm{Charge}_{\mathrm{HP}}[t] \tag{4.12}$$

When the optimization problem is formulated, it is then sent to the Gurobi solver. Gurobi provides an API that can communicate with Python, allowing users to interact with the solver programmatically. For linear optimization problems like this one, Gurobi employs the simplex algorithm. The simplex algorithm used by Gurobi applies an iterative search for the optimal solution. It makes small adjustments to the decision variables, systematically exploring the feasible region of the problem space to find the solution that maximizes or minimizes the objective function while satisfying all constraints. This iterative process continues until the optimal solution is found or a stopping criterion is met. The MIP gap indicates the level of optimality that the solver aims to achieve in finding the optimal solution. For this simulation, a MIP gap of 0.5% is used, meaning that the solver will terminate once it finds a solution where the objective function value is within 0.5% of the optimal solution. The linear programming problem is resolved utilizing the computational power of a Gurobi Cloud server, leveraging an AMD EPYC 7452 32-Core Processor with 16 physical cores.

4.3.1 Rolling Horizon Approach

The discretization of the CHP load points has introduced a total of 1.6 million dependent data points into the optimizer for a full-year simulation. Optimizing a full year would significantly increase computational effort. Therefore, a Rolling Horizon Approach is adopted. This approach segments the simulation into a finite number of optimizations, affecting the seasonal nature of the optimization. As a result, the optimization horizon no longer spans an entire year. To justify this simplification a year-long simulation is run, and the seasonal impact of storage is analysed.

The hypothesis implies that there isn't enough overcapacity available to fully engage in seasonal storage. During the summer, there's an opportunity to charge the storage with inexpensive heat, but these assets are already occupied providing the baseload. On the other hand, the electricity prices will be too low for the CHP to engage, which also doesn't align with the desire for renewable heat.

To validate this, testing is conducted, as shown in Figure 4.4. Here the distribution of staying time is included (4.4), where staying time refers to the time spent by a control volume in the storage. The distribution indicates the frequency at which a control volume remains in the storage for a certain duration. It can be observed that occurrences of storing time exceeding 600 hours are rare within a full year simulation.

Further analysis examines the average delta price of implementing larger storage capacities. It was found that there is a 30% increase in charging price when scaling up the storage capacity from 1 *GWh* to 20 *GWh*. As a result, the contribution of seasonal storage cycles can be neglected, justifying the use of a Rolling Horizon Approach.

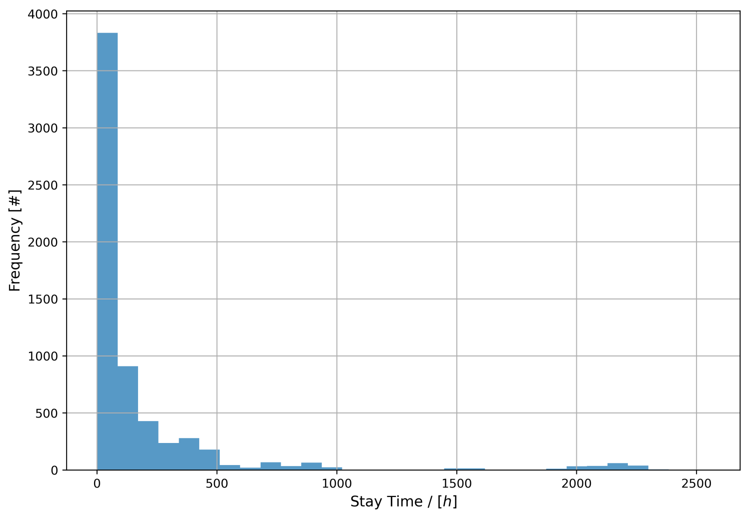

Figure 4.4: Time spent in storage per control volume

To integrate the Rolling Horizon Approach into the model, a simulation time span of one year is set, enabling us to capture the annual impact of the storage system. This extended time frame is crucial for accurately assessing the storage's performance over the course of a full year. With 8760 hourly data points, each interdependent on the others, substantial computational power is necessary. To optimize computational resources, we divide the optimization domain into 6 segments, each covering a 2-month period, with a 1-month overlap between adjacent segments. The overlap ensures that the optimization process remains continuous and preserves the integrity of the simulation. The 3-month interval aligns well with the mid-short-term storage strategy of this study.. Additionally, this approach acknowledges the absence of perfect forecasts and enables the model to approach dispatching strategies more realistically. By adopting this renewed strategy, a simulation time of one year within the hour is achieved, facilitating the evaluation of different storage capacities while optimizing computational efficiency.

4.3.2 Incorporating linear programming within the model

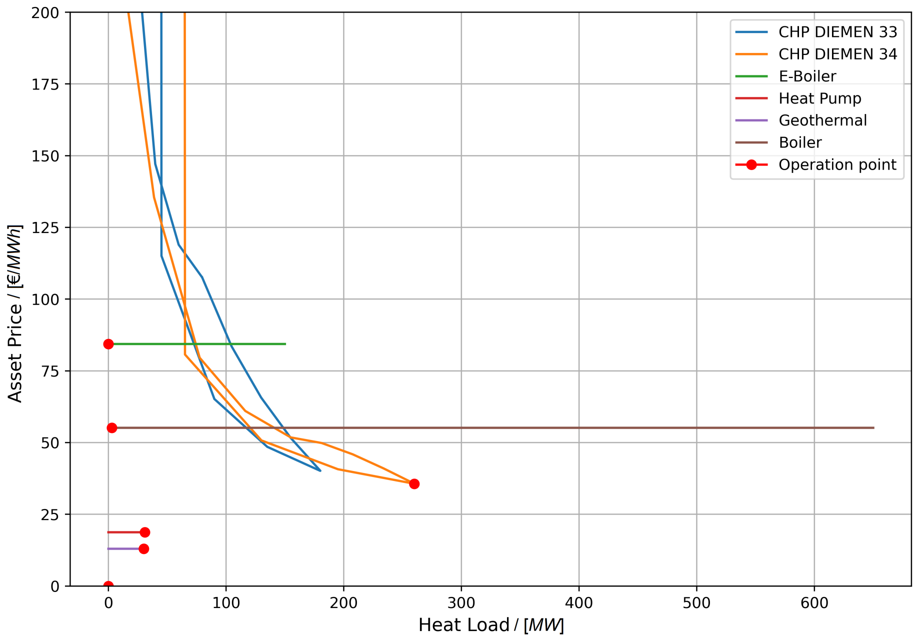

Figure 4.5: Correlation between asset price and Load

In Figure 4.5, the load dependency of assets is displayed. While for most assets the price of producing heat is independent of the load, CHPs (Combined Heat and Power) exhibit dependency on load. The figure illustrates the dispatch strategy for a time-step where the total heat load is 400 MW. The red dots indicate the chosen operational points for each asset determined by the linear programming approach. This analysis is conducted for a scenario where the electricity price is €60/MWh and the marginal costs of producing electricity are €105/MWh, resulting in a must-run situation where a loss is incurred on the produced electricity.

Three parameters influence the price of delivered heat in this scenario. Firstly, the efficiency, which is favorable when the electricity production is higher (P-Load), leads to lower prices of heat in the right top corner of the graph. Secondly, the load of electricity sets the price of heat. While the loss on the electricity market is linearly dependent, the price of heat rises faster at the top line than it does on the bottom line because of this reason. Thirdly, the produced heat is also a significant factor. As the losses made on the electricity market are spread out over the heat production, the heat prices are lower on the right of the graph than they are on the left. This price correlation is incorporated into the model as discrete set points.

Secondly, the charging and discharging strategy is tested. As an example, a typical summer day in 2040 is illustrated in figure 4.6 . During the summer, the heat load is particularly lower than the maximal capacity of the heat pump and geothermal energy combined. Therefore, the heat pump constantly charges the storage capacity (depicted in red), except for when the daily electricity peaks occur. Here, the storage capacity discharges, and the heat pumps are turned off (yellow line). The price of heat with and without thermal storage capacity is visualized in blue and orange, respectively. It can be observed that the storage flattens out the price of delivered heat.

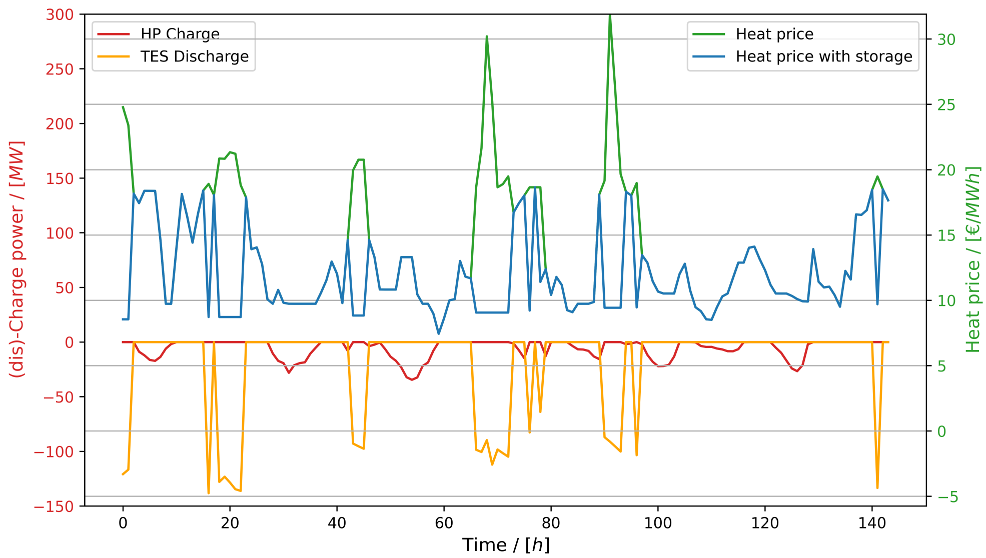

Figure 4.6: Week optimization in summer

4.4 Finite difference model

In this section the thermodynamical model of the stratified heat storage capacity is discussed, where stratified means that the storage consist of different layers with different temperature levels (see figure 4.7). to start with answering the question, why a detailed model of the storage capacity is needed and which constrains come into play. One of the key challenges of storing heat on the mid-short time domain, is the accompanied heat losses, which lead to economic and renewable energy losses. To describe the optimal storage control strategy a certain penalty for storing time should be introduced. The heat losses are related to the buffer's temperature and therefore linked to the State of Charge. Additionally, the model needs to address the changing temperature distribution within the buffer over time, this because the buffer is (dis)-charged on the last in, first out principle and influenced by thermal diffusion. This diffusion widens the "thermocline" within the buffer, contributing to exergy destruction. It's crucial to consider this, as layers dropping below the district heating network's supply temperature make stored heat ineffective. Complicating charging and discharging processes. Therefore, in addition to the optimization model, a thermodynamic model of the storage capacity is also developed.

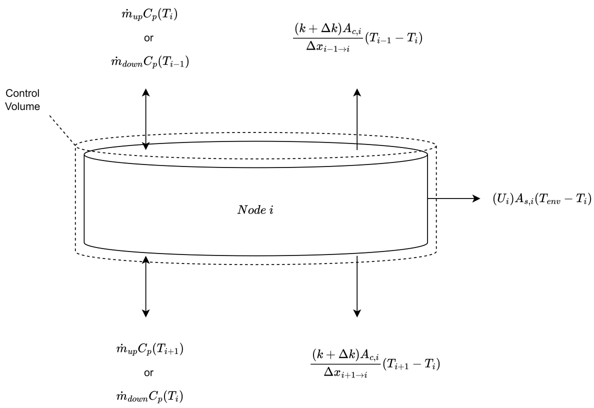

Figure 4.7: One dimensional controle volume

To obtain the temperature distribution this study makes use of a finite difference method, hereby the storage capacity is divided into certain amount of notes, which refer to an domain of equal temperature (see figure 4.7). Whereby the temperature difference is the driving force behind the heat diffusion. The literature available about stratified heat storage vessel's is diverse, ranging from 3-dimensional to 1-dimensional node schemes. With a fast converging model is preferred a 1-Dimensional approach is chosen. This should be enough to determine the heat loss and the temperature distribution.

The unsteady heat conduction equation has to be solved in an cylinderical cordinate system, which is intoroduced in equation 4.13. While heat flux is only expected to flow in the z direction $\frac{\partial}{\partial r}$ and $\frac{\partial}{\partial \phi}$ are equal to zero and no internal heat producation is assumed. This simplify the heat equation to 4.15, written in differential form. Here A is the cross-sectional surface, k and C_p stand for the thermal conductivity and heat capacity of water respectively.

$$\rho(\Delta x \Delta y \Delta z) C_p \frac{\partial T}{\partial t} = k \nabla^2 T + \dot{Q_v}''' \tag{4.13}$$

∇^2 for cylindrical coordinates depending on r, ϕ, z :

$$\nabla^2 = \frac{1}{r}\frac{\partial}{\partial r}\left(r\frac{\partial}{\partial r}\right) + \frac{1}{r^2}\frac{\partial^2}{\partial \phi^2} + \frac{\partial^2}{\partial z^2} \tag{4.14}$$

$$\rho A \Delta z C_p \frac{\partial T}{\partial t} = k \frac{\partial^2 T}{\partial z^2} \tag{4.15}$$

Now the thermal diffusion is defined the boundary conditions can be determined, to start with the heat-loss to the cylindrical walls. These walls contain of a steel a 10 *cm* (δ) polypropylene insulation layer, separated from the water and ambient air by two steel plates, here we neglect the thermal resistance of the steel plates. The insulation has a thermal conductivity of 0 .03 W/m K (k_{iso}). Further more the convective heat flux has to be defined, we will assume forced convection across a cylinder. While the convective heat transfer coefficient (h_θ) varies around the cylinder we will take a average heat transfer coefficient ($\bar{h_c}$). Therefore we will make use of a correlation which is derived from experimental data. First the Prandl number is calculated, which is 0.69 (-) for air. Matching the Nusselt number with the Reynolds numbers across a cylinder making use of empirical data. With the Nusselt number and the Reynolds number we can derive the average forced convection coefficient, this is displayed in equation 4.16. The average heat transfer coefficient ($\bar{h_c}$) with a wind velocity of 20 *m/s* is calculated as 35 W/m^2K. (Coimbra Mills [2015]).

$$\bar{h_c} = \frac{k\bar{N}u}{D} \tag{4.16}$$

To calculate the overall heat transfer coeficient (U) equation 4.17 is used. We now that at each node there is an equilibrium by the diffusive heat and the heat loss to the enviroment (know surface flux boundary condition), therefore we can add this to our heat conduction equation (4.15). This gives equation 4.18 which includes the heat loss, here S stands for the contact arrea by which heat is lost. Last the charging and discharging effect should be implemented into the energy balance, $\dot{m}$ stands for the massflow in or out the node multiplied by the heat capacity and temperature difference, for nodes in the middle this wil be the layers surounding them. Please note that equation 4.18 is for the middel layers, the first and N^{th} layer have a different surface area. Also because the are located a distance of $\frac{\Delta z}{2}$ from the surface the diffusion term is multiplied with $\frac{4}{3}$. To numerically solve te heat condutcion equation the differential equation has to be discretized, this is done making use of forward Euler. This finally yields Equation 4.19 as the discretized Fourier equation for middle notes.

$$\frac{1}{U} = \frac{1}{\bar{h_c}} + \frac{\delta_{iso}}{k_{iso}} \tag{4.17}$$

$$\rho C_p A \Delta z \frac{\partial T}{\partial t} = US(T_{amb} - T) + k\frac{\partial^2 T}{\partial z^2} + \dot{m}c\Delta T \tag{4.18}$$

$$T_i^{t+1} = T_i^t + \left(\alpha \frac{T_{i+1}^t + T_{i-1}^t - 2T_i^t}{\Delta z^2} + \beta \frac{T_{amb} - T_i^t}{\Delta z} + \dot{m}_{Charge} \frac{T_{i+1}^t - T_i^t}{\sigma} + \dot{m}_{Discharge} \frac{T_{i-1}^t - T_i^t}{\sigma} \right) \Delta t \tag{4.19}$$

Where Δz is the layer thickness and, (4.20)

$$\beta = \frac{U \cdot S}{\rho \cdot k \cdot A}, \quad \sigma = \rho \cdot A \cdot \Delta z \tag{4.21}$$

4.4.1 Results Thermal model

The thermodynamic model is integrated into the overall model to visualize the dynamics of the operated TES, providing insights into thermal diffusion and heat losses within the storage system. The evolution of the thermocline is illustrated first. The (dis)charging strategy obtained from the optimization model is fed into the thermodynamic model.

Figure 4.8 presents a 10-day snapshot of the heat storage modulation. The vertical axis represents the height of the storage, while the horizontal axis indicates time. The colormap displays the temperature distribution within the heat storage. The charging and discharging cycles are clearly visible, with the thermocline reaching a maximum of 10 meters. Additionally, the heat loss of the storage capacity ranges from 30 to 60 kW, showing a strong dependency on the state of charge. A constant outside temperature of 5 degrees Celsius is assumed, though factors like wind speed significantly influence the outside heat transfer coefficient.

In summary, these observations align closely with the operational data analyzed from the existing thermal energy storage systems.

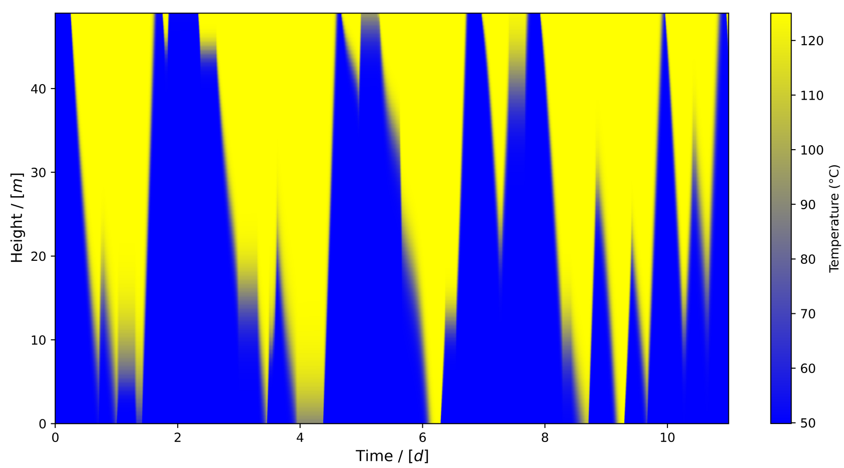

Figure 4.8: Heat map TES over time

4.5 Carbon footprint

To minimize the carbon footprint associated with produced heat, implementing heat storage serves as a secondary objective. This section outlines the methodology used to calculate the carbon footprint at different assets and timesteps within the model.

Starting with the peak boilers, which are gas-fired from 2030 to 2035. Subsequently, green hydrogen will replace natural gas as the fuel source. The carbon footprint (CFP) is measured in kg CO_2 per hour and is determined by multiplying the heat input from burning fuel Q in MWh by the specific emission factor (EMF) in kg_{CO_2}/MWh and then dividing by the coefficient of performance (COP). For peak boilers, the COP is considered as 1. The EMF represents the specific emissions per MWh of burnt fuel.

$$\mathrm{CFP}_{\mathrm{Boiler}} = \frac{Q \cdot \mathrm{EMF}}{\mathrm{COP}} \tag{4.22}$$

Secondly, the heat extracted from the CHP plant needs to be associated with a carbon footprint. The methodology for this is prescribed by the Dutch Ministry of Economics and Climate. When heat is extracted from a power plant, electricity production is sacrificed. Therefore, the sacrificed electricity production is theoretically equivalent to what would have been produced at a corresponding gas or coal power plant. This correlation is represented in Equation 4.23, where Q represents the heat of combustion and PL_{ratio} represents the sacrificed electricity production. The efficiency of producing electricity ($\eta_{\mathrm{elec.}}$) is assumed to be constant at 0.45.

$$\mathrm{CFP}_{\mathrm{CHP}} = \frac{\mathrm{Q} * \mathrm{PL}_{\mathrm{ratio}}}{\eta_{\mathrm{elec.}}} \tag{4.23}$$

Lastly, the power-to-heat assets need to be taken into account. They operate using electricity produced by another fossil or non-fossil-based production facility. The Dutch government has established a methodology for allocating carbon intensity to this used electricity, based on the Dynamic Reference Price Cap (DRP). This implies that when electricity prices are lower than the marginal cost of producing electricity in a gas or coal-fired plant (see Equation 4.3), the carbon intensity footprint of the used electricity is considered zero. This logic stems from the understanding that it would not be profitable to operate fossil-based production facilities at such times. This turning point is referred to as the DRP. When the electricity price is above the DRP, an averaged Carbon Emission Factor (EMF) is used, representing the average carbon intensity of the electricity mix over the course of a year. Table 4.4 presents the forecasted carbon emission factors that will be utilized in the model.

$$CFP_{HP/EB/GEO} = \frac{Q * EMF_{avg.}}{COP} \tag{4.24}$$

	year	2023	2030	2035	2040
EMF	t /MWh	0.27	0.09	0.07	0.05

Table 4.4: Forcasted yearly carbon intensity factor

The carbon intensity calculation is integrated within the optimization model. Since financial gains and carbon footprint have different units, a scaling factor is used in the objective function. The objective function imposes a penalty for charging the storage with sources that have high carbon intensity. This approach transforms the problem into a multi-objective optimization problem. By adjusting the scaling factor, the sensitivity of the solution can be fine-tuned.

5 Results

5.1 Introduction

Now that the model is established, the analysis can begin. The main objective is to answer the research questions, which are formulated to provide insights into how different storage capacities will affect various parameters within the district heating network. First, the model is validated (see 5.2) by comparing its decision-making and results with existing data. After validation, the model is set up for the scenarios outlined in Table **??**.

The core of the research focuses on how storage capacity can financially benefit this case study. Therefore, the first research question is dedicated to this aspect (see Chapter 5.3). Once this question is addressed, the study will focus on the capacity that provides the best results with regard to the first research question. The second research question investigates why this capacity is optimal and which variables contribute to its added value. This is analyzed through the influence of storage capacity on asset dispatch in Section 5.4.

Since the asset configuration is not constant over the modulation time and its effects vary, this aspect is addressed in Section 5.5. Closely related to this shift is the dependency on time. All input parameters are time-dependent, ranging from daily to seasonal to yearly variations. In section 5.6 the sensitivity to an alternative asset configuration is tested. Finally, the study examines carbon dependencies. District heating networks aim to decrease the carbon footprint of delivered heat, but the question remains whether this objective is met. This is discussed in paragraph 5.7.

Section's:

1. How will a growing storage capacity influence the reduced cost of delivered heat?
2. How will storage influence the dispatch of assets?
3. How will changing conditions over time influence the impact of storage?
4. How can financial and environmental benefits be optimized simultaneously?

Table 5.1: Projected Thermal Power (MW) per Source Type

Year	CHP (CH_4 /H_2) (MW)	E-boiler (MW)	Heat Pump (MW)	Geo-thermal (MW)	Boiler (CH_4 /H_2) (MW)
2023	440	–	–	–	650
2030	440	150	31	30	650
2035	440	150	41	80	730
2040	260	150	101	100	800

In Table **??**, the modeled configurations are presented, which simulates the transition from a fossil-based district heating network (DHN) to a Power-to-Heat system. This transition is implemented stepwise. The diverse asset configuration has a strong correlation with electricity prices. While heat loads are strongly dependent on seasonal variations, some loads are designed to be baseloads (operating more than 6000 hours a year), while others are intended to meet peak demands.

One point of interest is how the Combined Heat and Power (CHP) units are progressively transitioned from their role as baseload providers to mid-load providers. This shift raises the question of how thermal storage will interact during this transition. Specifically, how will the storage system support this shift and affect the operation and efficiency of the CHP units?

5.2 Validation

The first step in weighing the results is validation, achieved by comparing the outcomes with other district heating network simulation software. Vattenfall uses the C3PO model, which is inherently based on a linear programming optimization approach. Several fundamental differences need to be addressed.

First, regarding computational efforts, C3PO uses a far more detailed approach that includes thermo-hydraulic network descriptions. Consequently, the computational effort is significantly greater, with a typical year-long simulation converging in about six hours, whereas the proposed model converges within an hour. The intention was not to replicate the C3PO model entirely but to develop a fast-converging and fundamental model. Different project realization stages require varying levels of detail.This model not only converges quickly but also operates with more generalized data. For instance, no detailed network description is needed, as the heat load is described as a single sink.. Planning a C3PO run can take up to a month and requires substantial manpower in the modeling department, whereas this model is user-friendly and accessible to a broader user base within Vattenfall.

Secondly, this model employs a rolling horizon approach, which considers the inability to perfectly forecast pricing and heat load. In contrast, the C3PO program uses an ideal yearly forecast of all input variables. Additionally, this model uses a simplified asset configuration. The C3PO model accounts for a connection to a waste-burning facility (7.2% of total heat demand) and a small biomass-burning facility (2.0% of total heat demand). Furthermore, there are simplifications in the variable operational costs of the model.

By not modeling all heat assets the yearly heat load percentages do not fully add up, therefore the C3PO results are normalized to achieve a total of 100%. Additionally, hydraulic constraints influence dispatch, mainly in the winter when the system operates at full capacity. Finally, the C3PO model is a black-box model, meaning that certain parameters and data are not available. For instance, start-up costs and the coefficients of performance (COPs) for the heat pumps and geothermal assets are not published. This study relies on literature and commercially available data, which are assumed to align within acceptable limits.

Table 5.2: Validation results

Outcome	**Year 2030 (3200 *MWh*)**	**Year 2035 (3200 *MWh*)**	**Year 2040 (3200 *MWh*)**
CHP Dispatch			
Model	53.8%	30.1%	13.10%
C3PO	51.7%	34.7%	14.1%
Absolute Difference	3.0%	-4.60%	-1.00%
Relative Difference	9.9%	-15.3%	-7.6%
HP Dispatch			
Model	13.3%	13.8%	29.7%
C3PO	16.6%	14.3%	26.40%
Absolute Difference	-3.30%	-0.50%	3.30%
Relative Difference	-24.8%	-3.6%	11.1%
GEO Dispatch			
Model	13.3%	36.3%	38.1%
C3PO	15.2%	29.60%	41.0%
Absolute Difference	-1.9%	6.7%	-2.9%
Relative Difference	-14.3%	18.5%	-7.6%
EB Dispatch			
Model	18.30%	17.40%	10.7%
C3PO	13.1%	17.7%	8.7%
Absolute Difference	5.2%	-0.4%	2.0%
Relative Difference	28.4%	-2.3%	18.7%
BO Dispatch			
Model	2.10%	2.5%	8.40%
C3PO	2.5%	2.14%	5.9%
Absolute Difference	-0.4%	0.4%	2.5%
Relative Difference	-19.0%	14.4%	29.8%

In Table 5.2, the results of both models are compared for the three asset configurations simulated. The comparison begins with the dispatch of CHP units. It has been observed that these results are quite sensitive to the start-up costs considered. This sensitivity is particularly notable in the years 2035 and 2040 when the CHP is primarily performing as a mid-load unit, which explains the lack of consistent error across the simulated years.

The primary reason for the inconsistency in the geothermal dispatch error can be attributed to the simplification within the subsidy model. This model employs flat rates, and in the year 2035, the full-load hours of the geothermal installation exceed the subsidy cap, which ends at 6000 hours.

Generally, this model predicts a higher dispatch for the E-boiler. This discrepancy arises mainly because no fixed grid fees are implemented in the model, including the maximum monthly power capacity fees. This is partly because TenneT is reviewing this pricing structure to better align with the goals of the energy transition. This adjustment will mainly involve flexible grid fees, with the E-boiler expected to operate in the lower tariff domain.

Overall, the dispatch predictions of this model align with those from models like C3PO and fall within the resolution needed for this study.

5.3 Results for Question I: Correlation between Storage Capacities

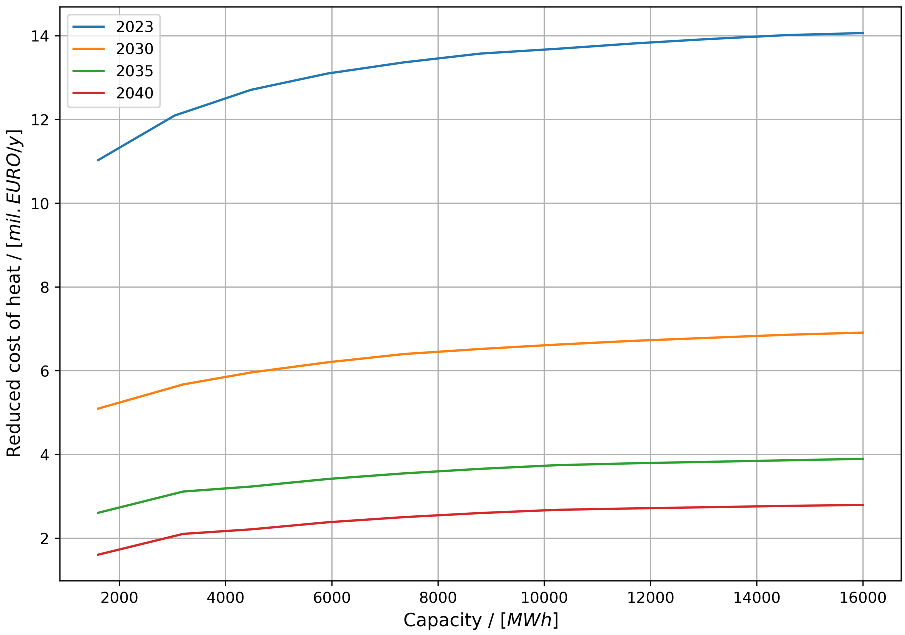

Figure 5.1: Simulation result differing years and capacities

The initial results addressing the correlation between larger storage capacities and cost reduction gains are presented in Figure 5.1. This figure demonstrates the performance of different heat source configurations with varying storage capacities. A significant initial gain is observed across all year simulations, followed by diminishing returns that follow a logarithmic trend and converge at an asymptote. The asymptote is determined by the overcapacity of assets during favorable hours. Consistent correlations between capacity and cost reduction are evident across all four simulations.

To investigate what this correlation is based on, a closer examination of the results for the smallest storage capacity (3200 *MWh*) is undertaken. This analysis aims to answer the question of why increased storage capacity delivers only marginal additional gains.

To understand the rapid initial increase resulting from smaller storage capacities, it is crucial to recognize that storage capacity should exploit periods when heat production is most cost-effective nd minimize production during expensive periods. This exploitation is limited by two factors: the storage capacity itself, which dictates how much overcapacity can be utilized, and the available overcapacity during these periods. Figure 5.1 suggests that storage capacity is not the limiting factor in this case. To visualize the overcapacity constrain, the heat load duration curve is shown in Figure 5.2 , which illustrates the number of hours the assets operate at certain loads. This curve helps visualize how different heating sources meet the varying heat demand over the year and highlights periods of overcapacity that can be harnessed using storage solutions.

It is evident that the heat baseload is primarily met by the geothermal source, as shown in Figure 5.2. The blue areas represent the dispatch of the geothermal source, operating at full load for 7000 hours without storage. Both GEO and HP assets serve as baseloads mainly due to their favorable COP. Without storage, there is considerable overcapacity for more than half of the year (Figure 5.2 a). Additionally, the CHP acts as a mid-load, supplementing the baseload as needed. It can be seen that the CHP is also always dispatched at maximum capacity with the implementation of storage (denoted in the figure with red).

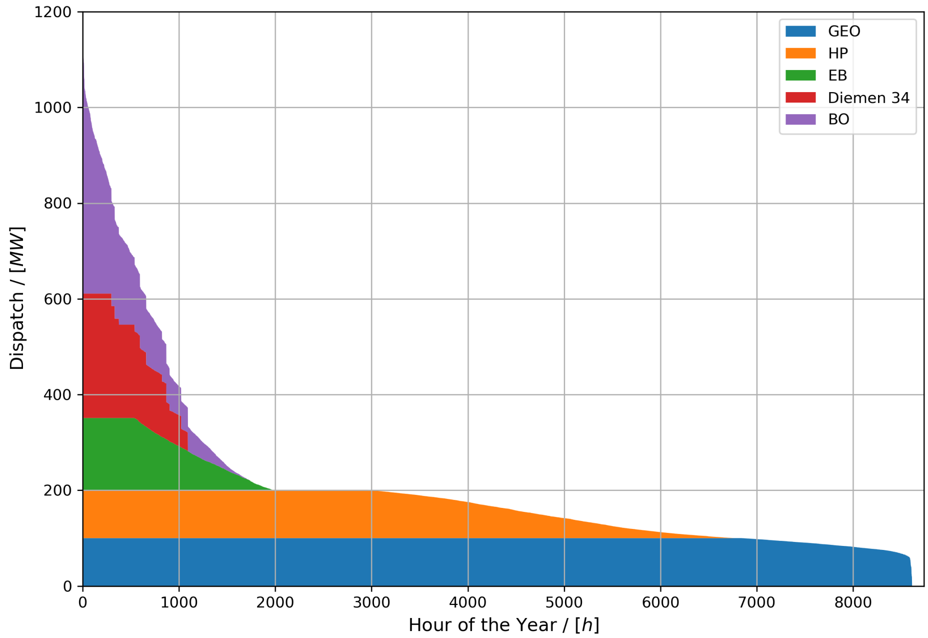

Figure 5.2: Load distribution curve without TES (2040)

The figure indicates that with even a small storage capacity, the assets almost always operate at full capacity. Running at full capacity is desirable because it maximizes heat production during favorable hours. The space between an asset's dispatch and its maximum dispatch is called overcapacity. A distinction must be made between desired overcapacity and general overcapacity. Due to the generally lower heat prices of heat pumps and geothermal assets, this overcapacity is usually desired, being the most cost-effective heat source.

For the CHP , the situation is more complex: some hours are far more expensive than others, making only certain hours of overcapacity desirable. The optimization strategy will determine which capacity is overall beneficial. For simplicity in this analysis, the hours where the CHP is already running are addressed as desired overcapacity.

In Figure 5.3 , it is shown how this overcapacity is utilized. For the heat pump and geothermal source, almost 70% of the full available capacity is used. The remaining 30% of inactive assets are due to seasonal heat demand; in the summer, there is overcapacity that is used to charge the storage. When prices are higher, the storage is discharged, happening on a daily basis. This additional overcapacity could be addressed with the implementation of seasonal storage, which is beyond the scope of this study but will be examined in the discussion. For the CHP, it can be seen that it operates at full capacity most of the time by implementing a storage capacity, this topic is further discussed in section 5.5.

Regarding the electric boiler (EB), there is available overcapacity that is not harvested. Even with increased storage capacity, this is not exploited, primarily due to its COP and the finite need for heat. Further conclusions on this topic are discussed in Section 5.4. Consequently, larger storage capacities do not further enhance the value of the TES, mainly because of the lack of favorable overcapacity and a finite heat load.

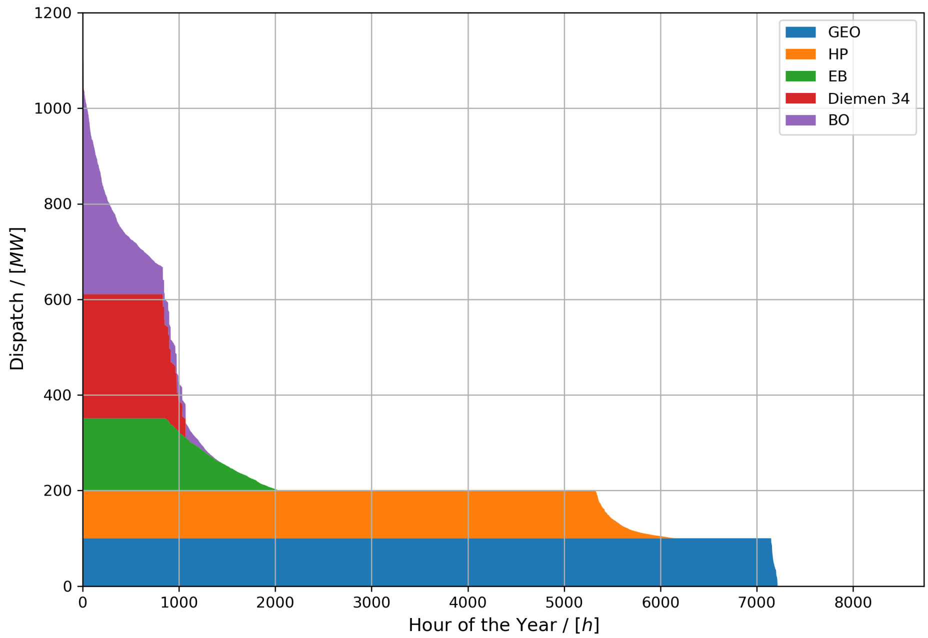

Figure 5.3: Load distribution curve with TES (2040)

5.3.1 Investment costs

Table 5.3: Investment case evaluation

Capacity (*MWh*)	Revenue a year (mil. €)				Cost (mil. €)	Pay-back (y)	
	2023	2030	2035	2040		2025-	2030-
1600	11.1	5.1	3.1	1.7	62	5.8	22.4
3200	12.1	5.7	3.8	2.1	96	10	not
Δ	1.4	0.6	0.7	0.3	34	not	not

To translate investment made into added value, an approach for describing the cost of the TES should be derived. This is done by comparing previously installed heat storage capacities within the industry. Generally, scaling up induces cost reductions per installed unit, so a scaling factor is needed. This is achieved using a process equipment scaling method, as displayed in equation 5.1. An R factor is determined based on scaling factors for large pressurized heat storage vessels. The value is then fitted to previous projects undertaken by Vattenfall, using the TES in Diemen (built in 2013) and a more recent project in Reuter, Germany (2020) as input variables. Both cases account for an indexation of 19 %, based on the cost rise between 2012 and 2020. The costs include all preparation, building, and development expenses, including the accumulator tank, pump station, and the cost of ownership. An R factor of 63 % is used based on Remer [1993]. These scaled investment costs can be seen back in table 5.3

$$\frac{\text{cost}_2}{\text{cost}_1} = (\frac{\text{size}_2}{\text{size}_1})^{\text{R}} \tag{5.1}$$

In Table 5.3, the financial metrics for 1600 *MWh* and 3200 *MWh* storage capacities are presented. The differences between these capacities, denoted as Δ, highlight the incremental gains from scaling up the storage. This comparison is essential as the revenue and costs do not scale linearly with increased storage capacity.

The returns vary significantly across different years, a phenomenon discussed in detail in Section 5.5. Additionally, the cost scaling is non-linear, showing a positive scaling trend. The main value of the storage is realized starting from the year 2023, with constant earnings assumed between the time steps. After the year 2040, the gains are kept constant based on the hypothesis that the asset configuration remains unchanged and the full energy transition is successful.

The pay-back period is analyzed under two scenarios: first, if the storage is built in 2025, the 1600 *MWh* capacity is recovered within the depreciation period of 30 years. This is also true if the storage is completed in 2030, although the payback period is considerably longer. For the 3200 *MWh* storage capacity, the payback times exceed the depreciation period, making this investment option unfeasible. In both scenarios, it would not be optimal to opt for the larger capacity, as denoted by Δ in Table 5.1, despite the positive effects of scaling costs.

5.4 Results of Question II: Influence of Storage on Asset Dispatch

While the heat storage capacity decouples real-time heat load and production, it introduces a time-based dependency. The objective of the storage capacity is to produce heat when conditions such as pricing and carbon footprint are favorable. As explained in Section 5.3, there are certain assets that can produce heat efficiently. When electricity prices are low, power-to-heat assets are advantageous. Conversely, when electricity prices are near the marginal cost of electricity production, the CHP becomes favorable. This is because the CHP can produce heat with a power-loss factor of 0.2 while it is already running. Additionally, there are more expensive assets, such as the electric boiler (EB) and gas boilers. On the other hand, the EB can dispatch its overcapacity during hours when electricity prices are low, optimizing its use.

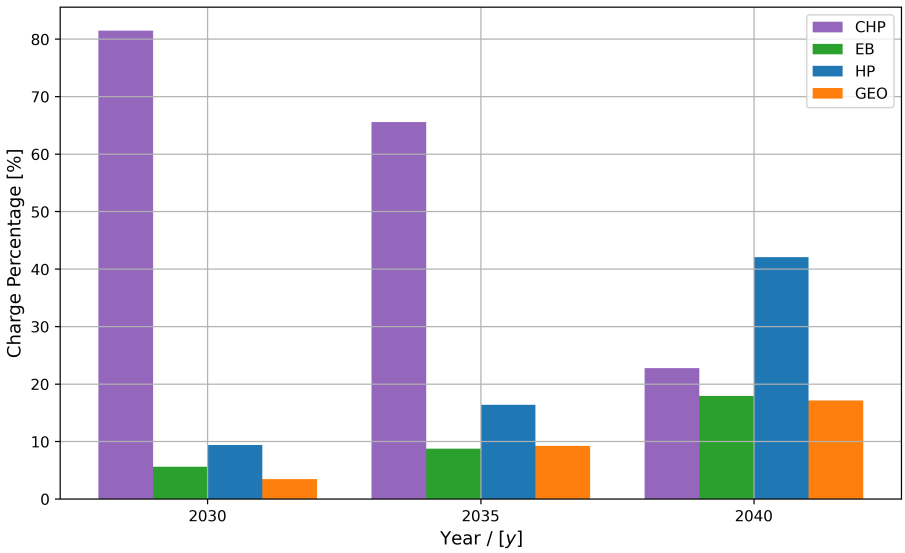

Figure 5.4: Overview of which asset charges the TES

Figure 5.4 illustrates the percentage of heat provided to the TES by each asset, the lighter/-darker bar represents the overcapacity without/with storage. It was anticipated that the TES would primarily be charged by the CHP and the less expensive power-to-heat sources, mainly because they operate at different pricing levels (power-to-heat around an electricity price of zero and CHP around its marginal costs). However, the actual ratio differed from the hypothesis. One reason for this is the overcapacity constraint discussed in the previous paragraph. Figure 5.5 presents the average overcapacity for each asset during hours of additional operation, ensuring that only the overcapacity at favorable hours is considered. It can be seen that a significant portion of the overcapacity is already utilized when using a 3200 *MWh* TES.

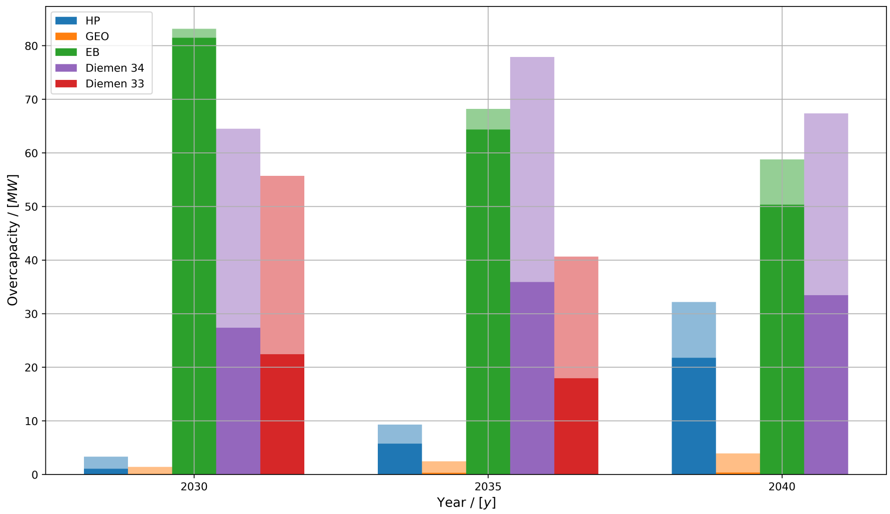

Figure 5.5: Overcapacity on assets

Another point of interest is the annual variability, which includes two aspects: first, the overcapacity per asset changes each year; second, the input variables and heat prices per asset vary annually. These topics will be further discussed in Section 5.5. One conclusion drawn is that the TES tends to charge with heat from the CHP.

Next, examine how the TES influences the dispatch strategy with and without storage. Figure 5.6 displays the asset dispatch for the year 2035. The first observation is that boiler dispatch is minimized, primarily because boiler heat is expensive, which is a logical outcome. However, what is unexpected is the reduction in the use of less expensive power-to-heat (P2H) sources when storage is implemented, while CHP dispatch increases. This is counterintuitive, as CHP is typically a more expensive asset than P2H sources. This suggests a non-linear correlation that necessitates further explanation.

This non-linearity arises from two factors. First, the efficiency of the CHP is non-linear, meaning that the optimization will prefer operating the CHP at full capacity. The second non-linearity occurs when the CHP operates at a loss in the electricity market, referred to as ”Out of the Money” . In this situation, the price of heat is derived from the loss made on the electricity market divided by the heat production. Since the capacity of the CHP is significantly larger than that of power-to-heat sources, the absolute cost reduction by running the CHP at its maximum capacity is substantial.

Although the CHP is more expensive than the HP and GEO, it is still dispatched because the heat load needs to be fulfilled. The absolute benefits from operating the CHP optimally far exceeds the gain from storing inexpensive heat generated by Geothermal and Heat-pump energy. This also explains why, in the initial years of the simulation with significant CHP dispatch, the gain from the TES is considerably larger.

H

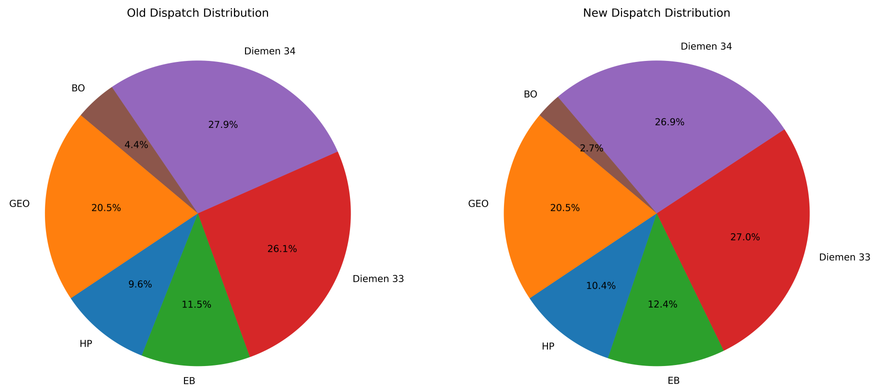

Figure 5.6: Asset dispatch 2035 (3200 *MWh* TES)

5.5 Results for Question III: How will changing conditions over time influence the impact of storage?

To fundamentally understand how the results of this model are derived, the influence of some key input variables must be addressed. The variables are dependent on time, so it's essential to examine how these dynamics within the modeling timeframe have influenced the final results.

Firstly, consider the evolution of electricity prices. The electricity price is one of the most influential input parameters. It is important to note two key points: power-to-heat sources benefit from low electricity prices, while CHPs perform best around their marginal cost. The marginal cost of producing electricity shifts during the simulation period, after a increase in 2035 due to higher carbon taxation a decline is expected in 2040. This was quite surprising, considering hydrogen is generally seen as an expensive fuel. However, in the year 2035, carbon emission bonds significantly influence the cost.

In Figure 5.7, the daily heat mix for the year 2040 is displayed. Geothermal and heat pump assets primarily provide the baseload. During the summer, the overcapacity of the geothermal source is used to charge the storage, and the TES is then dispatched during less favorable hours. The CHP and E-boiler mainly fulfill their roles as mid-load sources, supplementing the baseload when needed. These two assets compete based on price; during higher electricity prices in the winter, the CHP is preferred over the E-boiler. In autumn and spring, the E-boiler often serves as a baseload source.

It is important to consider the daily price fluctuations, which are mainly driven by demand. Prices are generally higher every morning and afternoon, set by fossil fuel-based power plants when no renewable energy is available. This implies that the CHP will generally have an opportunity to produce heat on a daily basis.

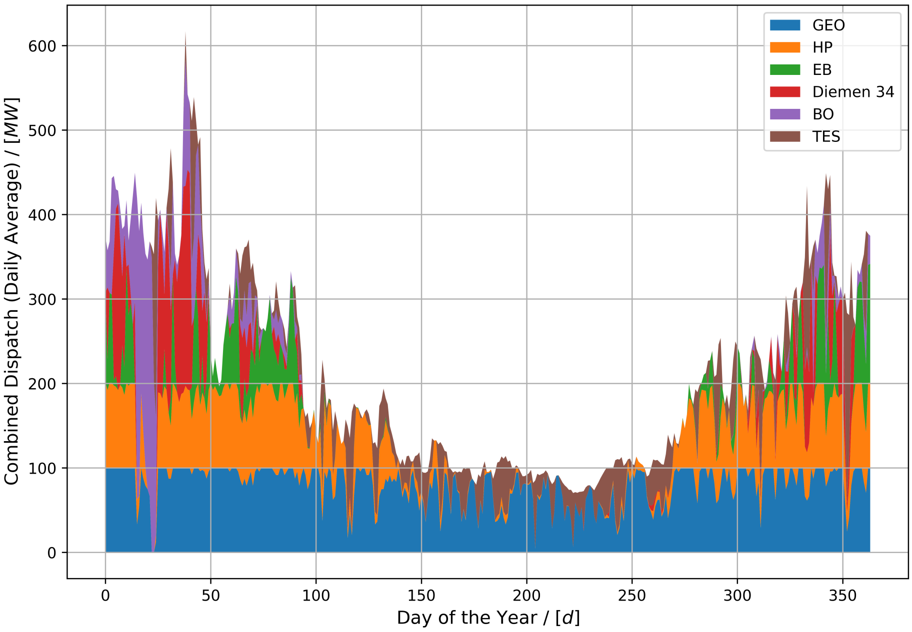

Figure 5.7: Daily average energy mix 2040

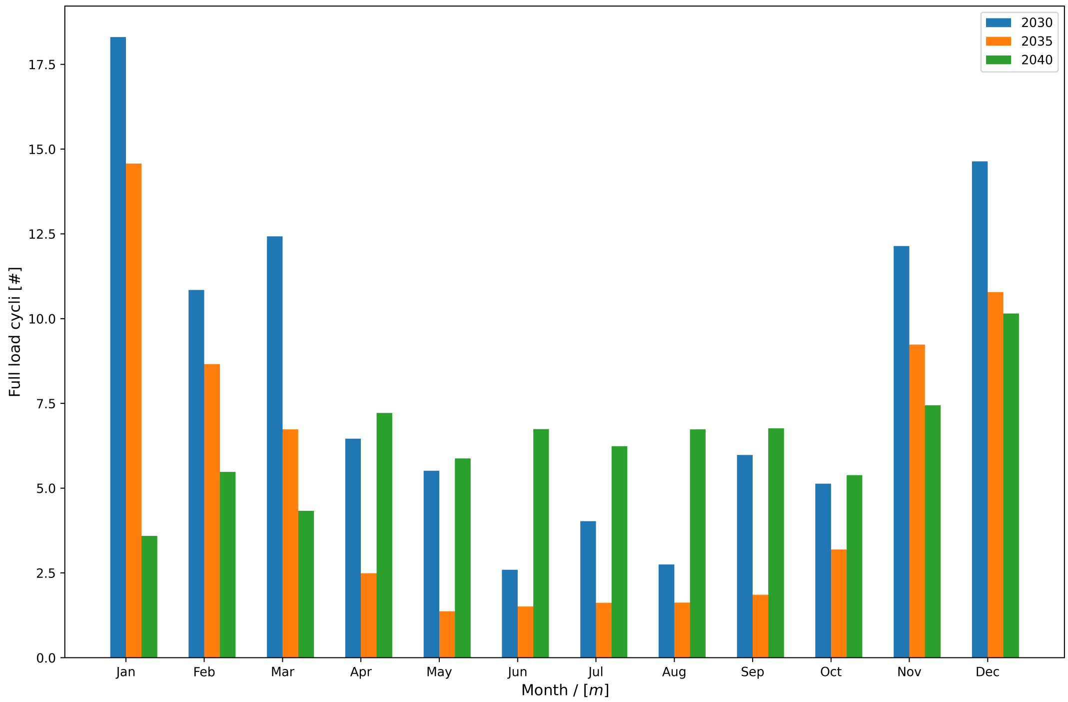

Figure 5.8: Full-load cycli per month

The first aspect of time variability to be addressed is the differences within a simulation year. Understanding where and why value is created is crucial. Figure 5.8 displays the number of full load cycles the TES completes each month of the year. The dispatch is dependent on two previously addressed factors: overcapacity and favorable charging conditions.

In the first year, the main value of the TES is realized in the winter, primarily because there is overcapacity, and the CHP prices are strongly influenced by electricity price fluctuations. In the summer, there is no overcapacity available for the power-to-heat assets, and therefore, the CHP operates at full capacity for a few hours in the morning.

By 2040, full load cycles are predominantly completed in the summer due to the overcapacity generated by the power-to-heat sources. During the winter of 2040, the TES is not used as frequently because Diemen 33 has been decommissioned, resulting in a significant reduction of overcapacity while the heat load continues to grow. This illustrates that the influence of the asset configuration on the value generated by the TES is highly dependent on these factors.

5.6 Results for Question IV: Sensitivity study

The asset configuration for this study is based on a setup with relatively low operational costs. This is due to the favorable COPs (Coefficients of Performance) of baseload assets, which are operationally and environmentally advantageous. However, this configuration heavily relies on subsidies, raising the realistic question: What will happen if the proposed asset configuration is not realized?

One option to consider, while still aiming to transition to a power-to-heat-based scenario, is to increase the planned E-boiler capacity. This analysis focuses on the year 2040, as this will be the year when Diemen 33 is decommissioned, highlighting the real need for additional capacity.

Table 5.4: Alternative asset configuration

Year	**CHP** [CH_4 /H_2] (MW)	**E-boiler** (MW)	**Boiler** [CH_4 /H_2] (MW)
2040	260	600	800

The overall conclusion of this study thus far is that a lack of overcapacity primarily limits the value generated by the storage capacity. To further address the sensitivity of this parameter, an alternative asset configuration is tested (see Table 5.4). An E-boiler with an overcapacity of 600 MW is installed. Due to the unfavorable COP of the E-boiler and the prices being far from the CHP's optimal range, the value of the storage is expected to increase.

Figure 5.9 shows that this is indeed the case (bar 2040 alt.). The higher absolute price differences of heat at certain hours lead to an increased value of the TES. However, the operational expenditures (OPEX) in general are significantly higher with this asset configuration. On the other hand, the investment costs for the E-boiler are considerably lower. This study primarily focuses on a fixed asset configuration strategy, excluding investment optimization.

Two extreme points are chosen: first, a system with diverse assets including heat pumps with favorable COPs, and second, a system with only a CHP and an E-boiler with overcapacity. An interesting future optimization problem would be to optimize the total investment including operational costs. This topic will be reserved for further studies.

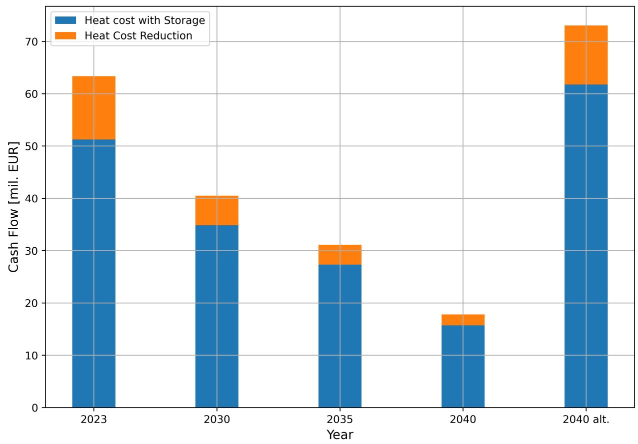

Figure 5.9: Heat cost alternative asset configuration

5.7 Results for Question V: How can financial and environmental benefits be optimized simultaneously?

In the final section of the results, the effect of a multi-objective optimization is tested, focusing on both financial gains and carbon footprint reduction in operating the thermal storage. The dispatch planning of the assets is inherently optimized based on pricing, but the buffer employs a multi-objective function to achieve both goals simultaneously. The buffer capacity is restricted to 3200 *MWh* to align with the primary goal of reducing heating costs. The model was run for a 50-day span in winter, as this period typically has the highest carbon footprint, offering the most potential for optimization. The optimization was performed by adjusting a scalar variable that weighted the influence of financial and environmental impacts in the objective function.

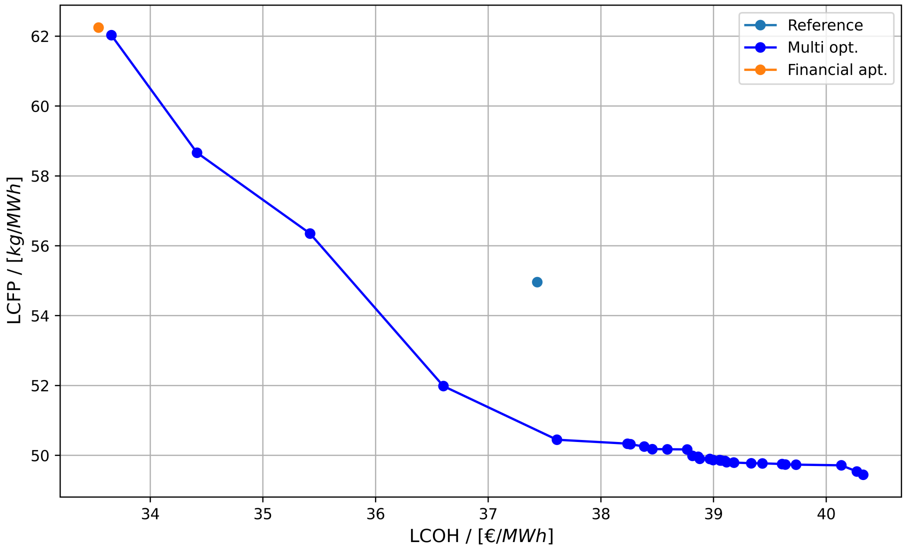

Figure 5.10: Pareto front: Financial and Environmental benefits

Figure 5.10 represents a Pareto front plot illustrating how the optimization of financial and environmental gains are related. The results are displayed as the Leverage Cost of Heat (LCOH) and the Leverage Carbon Footprint (LCFP). The light blue dot represents a district heating network without storage, the orange dot represents purely financial optimization, and the blue dots represent the results of multi-objective optimization. The first notable observation is that the carbon footprint increases as financial benefits increase. This is due to the higher dispatch of CHP power. According to Dutch regulations, the carbon footprint of producing heat with a CHP is calculated with a fixed plant efficiency. Therefore, the gains from running the CHP at maximum capacity do not result in a lower carbon footprint.

When electricity prices are below the Dynamic Reference Price (DRP), a carbon footprint of zero is assigned to the P2H sources. When prices are above the DRP, a carbon footprint of 70 *kg/MWh* of used electricity is assigned. For the CHPs, a constant carbon footprint of

83 *kg/MWh* is assigned, and for the boiler, it is 226 *kg/MWh*. Why can't the storage further reduce the carbon footprint? Mainly because, in winter, there are extended periods where electricity prices are above the DRP, and the heat load is high, causing the system to operate at maximum capacity.

The improvements in carbon emissions are most significant in the winter, primarily achieved by reducing the dispatch of the gas boilers. Due to the coefficient of performance (COP) and the low DRP in summer, the absolute gain in carbon footprint reduction is relatively low during this season, partly because the electricity price is not much above the DRP. In winter, the carbon footprint can be decreased by 20% without negatively affecting the cost of produced heat. The cost of reducing the carbon footprint by shifting away from the financial optimum follows a linear trend initially. To decrease the carbon footprint by 1 *kg*, the cost of heating increases by 0.3 euros. This is a significant amount compared to the emission trading system, where it only costs 0.1 euros per *kg* in 2035. Additionally, the lack of overcapacity remains an issue, even from the storage capacity perspective.

6 Conclusion

The core of this study focused on the financial optimization of Amsterdam's district heating network, with a special emphasis on sensible heat storage. The results of the first research question reveal how storage financially benefits the district heating of Amsterdam. Following this, several phenomena were highlighted to explain why a particular storage capacity performs as it does. With this understanding, final conclusions be drawn and general rules that may help in better understanding and designing new generation district heating networks.

First, the added value of scaling up storage capacity shows a logarithmic correlation with its realized value. The optimal value in this study was found to be 1600 *MWh*. The financial benefits vary from 11.1 million euros in 2023 to 1.7 million euros in 2040, with the payback time ranging from 5.8 years to 22.4 years, depending on when the storage is commissioned between 2024 and 2030. Scaling up the storage to 3200 *MWh* does not result in positive financial benefits that can be paid back through revenues. The results indicate that the daily fluctuations in heat prices are utilized most effectively. While there are also weekly and seasonal heat price fluctuations, there is no overcapacity to harvest these trends.

One of the key lessons learned about the transformation towards a 4th generation district heating network is the role the CHP plays. With higher penetration of renewable energy, electricity prices will more frequently fall below the marginal cost of electricity. Initially, the CHP acts as a baseload in the early years of the "warmte-transitie" (heat transition). It is evident that when operating below the marginal cost, the CHP price is negatively and non-linearly correlated with the heat produced. Therefore, in the early years of this transition, the value of storage capacity is mostly gained by optimizing the CHP dispatch.

Additionally, it was observed that operationally inexpensive power-to-heat loads provide a baseload, which is not designed to fill the storage. A storage could eventually have a decreasing effect on power-to-heat sources due to the non-linear gain observed by running the CHP at its maximum capacity. The storage is mainly utilized by optimizing the dispatch of mid-load assets, like the E-boiler and the CHP. The heat load is strongly seasonal, enabling the heat pump to act as a mid-load in the summer, fully dispatching and charging the storage when abundant renewable energy is available.

This study examined the transition from a fossil-based district heating network to a power-to-heat fed system. The findings suggest that in a fully developed power-to-heat system, the value of storage minimizes. This is due to a lack of overcapacity and the favorable COPs of assets, which lower the absolute returns for storage. Thus, pressurized heat storage capacity becomes difficult to justify financially. Storage becomes interesting when there is a midload available in winter with relatively high costs, which could occur if fuel or electricity costs rise.

With regard to the environmental impact of storing heat, the first conclusion is that heat storage can decrease the carbon footprint in winter by up to 20% without affecting the cost of produced heat. In summer, no significant benefits can be achieved since the electricity prices are most of the time below the DRP benchmark. The correlation between sacrificing financial gains and improving the carbon footprint is initially linear, with a slope of 0.3 euros per saved *kg* of CO_2 observed.

In conclusion, this study is based on long-term pricing forecasts, which inherently come with a degree of uncertainty. However, one thing is clear: a heat storage system contributes to a more robust energy system, making it less vulnerable to variables outside Vattenfall's control, such as fuel prices, electricity prices, and subsidies. The term ”warmte transitie” includes ”transition,” and transitions are set in motion by disrupting the norm.

7 Discussion

In the discussion, the conclusions from the previous chapter are examined in an academic context, highlighting the literature gap. While many studies have focused on district heating networks combined with thermal storage, this study emphasizes the gradual shift of an existing network from a fossil-based system to a power-to-heat system. Additionally, it explores the diverse mix of power-to-heat assets, investigating the separate effects of storage, heat pumps, E-Boilers, and CHP plants. These assets have dependencies on their dispatch and interaction with heat storage, but this study also identifies other correlations.

Furthermore, a full-year simulation was conducted, which included seasonal influences on heat load. This primarily affected the overcapacity in summer Vs. winter, which could be utilized for thermal energy storage.

CHP and Thermal Storage Integration

Several studies have examined the effects of heat storage combined with extraction condensing steam turbine plants. This study delves into how the CHP plant is modeled, focusing on the description and linearization of its non-linear parts. Two main approaches are used:

1. **Single-Entity Approach:** In this method, the CHP is treated as one entity where costs are defined as the fuel costs written within the convex domain of the PQ diagram. This method deals with the semi-continuity of the convex cost function using the big M method.
2. **Separate Production Costs Approach:** Here, the costs of heat and electricity production are considered separately, introducing a non-linear dependency on the heat load. This can be fixed by prescribing preset operational points using binary decision variables.

When reviewing literature, the single-entity approach is often preferred as it reduces non-linearities. However, this study's approach is more suitable for optimizing configurations with multiple assets, assigning a distinct price to heat. Both methods ultimately present similar results, but this study's method is more computationally intensive. Never the less payback times for integrating thermal storage and optimizing CHP dispatch are observed within one year, heavily dependent on asset configuration and investment costs. Additionally, a logarithmic trend is seen with increasing storage capacity. Cost saving of 18.2 precents are observed by

The main conclusions of implementing thermal energy storage (TES) with regard to a CHP are that it significantly affects the operational hours of the CHP. The TES enables the CHP to run at full capacity under favorable conditions (Benalcazar and Kamiński [2021]). Additionally, it was found that the use of peak boilers was minimized in the asset configuration that included both TES and peak boilers. Benalcazar [2021] conducted a case study on a single CHP and a 400 *MWh* TES, which in 2020 led to cost savings of 0.65 million euros by including the TES.

Impact of Thermal Energy Storage in Power-to-Heat Systems

The second topic examines how implementing thermal energy storage influences the shift to a power-to-heat-based system. Other studies have verified that including power-to-heat sources with favorable Coefficients of Performance (COPs) can serve as a base load. However, this is highly dependent on electricity and fuel prices. This study found that as the share of power-to-heat sources grows, the E-Boiler is used less frequently, primarily due to the more favorable COPs of other sources such as the CHP in winter and heat pumps and geothermal energy in summer. Sinha et al. [2019] studied how the flexibility of a DHN can be improved by introducing an electric boiler. There is a limited availability of full-year, multi-asset, techno-economic studies. Therefore, this study contributes by filling this gap.

.

8 Recommendations

One of the main recommendations within this thesis is to avoid specifying the cost of heat separately when modeling the CHP (Combined Heat and Power). Doing so introduces non-linearities, which significantly increase the complexity of the model. For optimization tasks, a model that converges quickly is beneficial. While this thesis focuses on optimizing an existing asset configuration strategy, future models could also include CAPEX costs. This would help find the best investments for expensive assets like geothermal systems and heat pumps.

Additionally, this study used a perfect forecast with a rolling horizon approach. It is important to further investigate the sensitivity of the model to these input variables. Understanding how policy changes, such as carbon taxes or shifts in electricity prices, affect the model is crucial. For example, the influence of different energy mixes, like a shift to more nuclear power or an increase in flexible power sources like batteries and electrolyzers, should be explored. Implementing different scenarios based on these external factors would provide a better understanding of potential outcomes.

Another point to consider is the approach of assuming a perfect forecast. In reality, both prices and heat demand are influenced by the accuracy of weather forecasts. Further research should investigate the sensitivity of the model to these forecasting inaccuracies. Moreover, additional markets where assets can participate, such as the net balancing market for electric boilers or CHP plants, should be included in the model for a more comprehensive daily planning of assets.

The use of a pressurized buffer should also be reconsidered. Currently, it is necessary due to the high supply temperatures of the heating network, avoiding the need for auxiliary devices. However, by 2035, it is likely that supply temperatures will be lowered below the boiling point at atmospheric pressure, potentially eliminating the need for a pressurized buffer.

Finally, it is evident that there will be an overcapacity of power-to-heat sources during the summers starting from 2040. While this study did not delve into seasonal optimization, future research should explore better ways to utilize this overcapacity.

Additionally, the role of the CHP (Combined Heat and Power) system in a power-to-heat (P2H) setup needs further evaluation. The energy transition puts the role of CHPs under pressure, mainly due to the decrease in full load hours for CHPs and the competition from power-to-heat sources. This dynamic should be thoroughly examined in future research to understand the evolving role of CHPs in the energy landscape.

9 Appendix A

In this appendix, several Python code snippets are provided to help further understand the modeling approach used in this study. These snippets illustrate key components of the model, including the objective functions and constraints, which are implemented using the Pyomo optimization library. The provided code can serve as a reference for replicating or extending the model for similar applications.

```
def objective_func(model):
    # sum the price times power produced for all time steps
    return sum([model.load_CHP[t]*model.price_CHP[t]+model.load_HP[t]*model.price_HP[t]+model.load_EB[t]*model.price_EB[t]+model.load_BO[t]*model.price_BO[t] for t in model.T])
model.objective = pyomo.Objective(rule=objective_func, sense=pyomo.minimize)
```

Listing 9.1: Objective function dispatch strategy

The code above defines the objective function for the dispatch strategy, minimizing the total cost by summing the price times the power produced for all time steps.

```
def objective_func(model):
    # sum the price times power produced for all time steps
    return sum([model.TES_discharge[t]*model._price_without_storage[t] - model.charge_CHP[t]*model.price_CHP[t] - model.charge_EB[t]*model.price_EB[t] - model.charge_HP[t]*model.price_HP[t] for t in model.T])

model.objective = pyomo.Objective(rule = objective_func, sense=pyomo.maximize)
```

Listing 9.2: Objective function storage controll

The snippet above defines the objective function for storage control, maximizing the benefits of storage by considering the discharge and charging costs across different assets.

```python
def constr_store_balance(model, t):
    if t == 0:
        # initial inventory of storage at time 0
        return model.s[t] == 0 - model.TES_discharge[t] + model.charge_CHP[t]+ model.charge_EB[t] +model.charge_HP[t]
    else:
        return model.s[t] == model.s[t-1] - model.TES_discharge[t] + model.charge_CHP[t] + model.charge_EB[t] + model.charge_HP[t]

model.constr_store_balance = pyomo.Constraint(model.T, rule=constr_store_balance)
```

Listing 9.3: Constraint for storage balance definition in Python

The above code snippet defines the storage balance constraint, ensuring that the storage inventory is updated correctly over time based on the discharges and charges from various sources.

```
def CHP_price(price,P_Load):

    eta_elec = Electric_eff(P_Load)
    Fuel_heat_flow = Heat_loss_ratio/eta_elec
    Fuel_elec_flow = 1/eta_elec
    Fuel_heat_cost = Fuel_heat_flow*Gas_price
    Fuel_elec_cost =  Fuel_elec_flow*Gas_price
    Tax_heat = Fuel_heat_flow*CO2_emmision_gas*Carbon_tax_2023
    Tax_elec = Fuel_elec_flow*CO2_emmision_gas*Carbon_tax_2023

    Marginal_heat = Fuel_heat_cost+Tax_heat
    Marginal_elec = Fuel_elec_cost+Tax_elec

    C = [Marginal_elec,Marginal_heat]
    O = [0,0]
    A = [0,(Marginal_heat+Marginal_elec*Heat_loss_ratio)]

    # If x is a single value, calculate the price
    if isinstance(price, list):
        price_CHP = [round(linear_line(A, C)(p), 2) if p < Marginal_elec
             else round(linear_line(O, C)(p), 2) for p in price]
    else:
        price_CHP = round(linear_line(A, C)(price), 2) if price <
            Marginal_elec else round(linear_line(O, C)(price), 2)

    return (
        price_CHP,
        round(Marginal_elec, 2),
        round(Marginal_heat, 2)
    )
```

This final snippet provides a function for calculating the price of CHP-generated heat and electricity, incorporating various factors such as fuel costs, emissions, and taxes.

Bibliography

Gabin Mantulet *Carbon price forecast under the EU ETS*; 2023.

Guelpa, E.; Verda, V. Thermal energy storage in district heating and cooling systems: A review. **2019**,

Brouwer, A. S.; van den Broek, M.; Seebregts, A.; Faaij, A. Operational flexibility and economics of power plants in future low-carbon power systems. *Applied Energy* **2015**, *156*, 107–128.

United Nations Key aspects of the Paris Agreement. 2015.

INTERNATIONAL ENERGY AGENCY *Energy Technology Perspectives 2012*; 2012.

Statista Number of heat pumps in operation in the Netherlands from 2013 to 2020. 2021.

CBS *Energy consumption private dwellings; type of dwelling and regions*; 2023.

Tennet *Maandelijkse updates over congestie*; 2023.

Vattenfall NV *Anual report 2022*; 2023.

Abdur, R.; Mazhar, S.; Liu, Shukla, A. A state of art review on the district heating systems. **2018**,

Gong, M.; Werner, S. Exergy analysis of network temperature levels in Swedish and Danish district heating systems. *Renewable Energy* **2015**, *84*, 106–113.

Skagestad, B.; Mildenstein, P. *District heating and cooling connection handbook*; NOVEM, Netherlands Agency for Energy and the Environment, 2002.

Vattenfall AB *Green Heat dpt*; 2024.

Lund, H.; Werner, S.; Wiltshire, R.; Svendsen, S.; Thorsen, J. E.; Hvelplund, F.; Mathiesen, B. V. 4th Generation District Heating (4GDH). Integrating smart thermal grids into future sustainable energy systems. 2014.

Zakeri, B.; Staffell, I.; Dodds, P.; Grubb, M.; Ekins, P.; Jääskeläinen, J.; Cross, S.; Helin, K.; Castagneto-Gissey, G. Energy Transitions in Europe – Role of Natural Gas in Electricity Prices. *SSRN Electronic Journal* **2022**,

Oosthuizen, A. M.; Inglesi-Lotz, R.; Thopil, G. A. The relationship between renewable energy and retail electricity prices: Panel evidence from OECD countries *. **2021**,

Bhatia, K.; Mittal, R.; Varanasi, J.; Tripathi, M. M. An ensemble approach for electricity price forecasting in markets with renewable energy resources. **2021**, Meng, A.; Wang, P.; Zhai, G.; Zeng, C.; Chen, S.; Yang, X.; Yin, H. Electricity price forecasting with high penetration of renewable energy using attention-based LSTM network trained by crisscross optimization. *Energy* **2022**, *254*.

Martín-Rodríguez, G.; Cáceres-Hernández, J. Modelling the hourly Spanish electricity demand.

Hagfors, L. I.; Kamperud, H. H.; Paraschiv, F.; Prokopczuk, M.; Sator, A.; Westgaard, S. Prediction of extreme price occurrences in the German day-ahead electricity market. *Quantitative Finance* **2016**, *16*, 1929–1948.

Bunn, D.; Andresen, A.; Chen, D.; Westgaard, S. Analysis and Forecasting of Electricity Price Risks with Quantile Factor Models. *The Energy Journal* **2016**, *37*.

Pariente-David, S. *The Cost and Value of Renewable Energy: Revisiting Electricity Economics*; p 21.

Bert den Ouden *Electrification in the Dutch process industry*; 2017.

Gonzalez-Salazar, M.; Klossek, J.; Dubucq, P.; Punde, T. Portfolio optimization in district heating: Merit order or mixed integer linear programming? *Energy* **2023**, *265*, 126277.

European Comission *Questions and Answers on the revised EU Emissions Trading System* ; 2008.

Dan Williams Emissions Trading Scheme – auctions and how they work. 2021.

Our World in Data *Carbon dioxide emissions factors*; 2023.

Le Sko, M.; Bujalski, W.; Futyma, K. Operational optimization in district heating systems with the use of thermal energy storage. **2018**,

Fernandez, A. I.; Martnez, M.; Segarra, M.; Martorell, I.; Cabeza, L. F. Selection of materials with potential in sensible thermal energy storage. *Solar Energy Materials and Solar Cells* **2010**, *94*, 1723–1729.

Cruickshank, C. A.; Baldwin, C. Sensible thermal energy storage: diurnal and seasonal. **2022**,

Thomsen, P. D.; Overbye, P. M. Advanced District Heating and Cooling (DHC) Systems Energy storage for district energy systems. **2016**,

Dahash, A.; Steingrube, A.; Elci, M. A Power-Based Model of a Heating Station for District Heating (DH) System Applications. Proceedings of the 12th International Modelica Conference, Prague, Czech Republic, May 15-17, 2017. 2017; pp 415–424.

Li, H.; Hou, J.; Tian, Z.; Hong, T.; Nord, N.; Rohde, D. Optimize heat prosumers' economic performance under current heating price models by using water tank thermal energy storage. **2021**,

Xu, J.; Wang, R.; Li, Y. A review of available technologies for seasonal thermal energy storage. **2013**,

Jayathunga, D. S.; Karunathilake, H. P.; Narayana, M.; Witharana, S. Phase change material (PCM) candidates for latent heat thermal energy storage (LHTES) in concentrated solar power (CSP) based thermal applications - A review. 2023.

J.F.C. Flores, J. C. V. M. B. L., A.R. Espagnet Techno-economic assessment of active latent heat thermal energy storage systems with low-temperature district heating. *Sustain Energy Plann Manage* **2017**, *13*, 5–18.

N'Tsoukpoe, K. E.; Liu, H.; Le Pierrès, N.; Luo, L. A review on long-term sorption solar energy storage. *Renewable and Sustainable Energy Reviews* **2009**, *13*, 2385–2396.

Akorede, M. F.; Hizam, H.; Pouresmaeil, E. Distributed energy resources and benefits to the environment. 2010.

Mago, P. J.; Fumo, N.; Chamra, L. M. Performance analysis of CCHP and CHP systems operating following the thermal and electric load. *International Journal of Energy Research* **2009**, *33*, 852–864.

Michael Goll *COMBINED HEAT AND POWER (CHP) GENERATION*; 2017.

Milan, C.; Stadler, M.; Cardoso, G.; Mashayekh, S. Modeling of non-linear CHP efficiency curves in distributed energy systems.

Koç, Y.; Yağlı, H.; Görgülü, A.; Koç, A. Analysing the performance, fuel cost and emission parameters of the 50 MW simple and recuperative gas turbine cycles using natural gas and hydrogen as fuel. *International Journal of Hydrogen Energy* **2020**, *45*, 22138–22147.

Kumar, N.; Besuner, P.; Lefton, S.; Agan, D.; Hilleman, D. *Power Plant Cycling Costs*; 2012.

Decoussemaeker, P. *Startup time reduction for Combined Cycle Power Plants 8 th International Gas Turbine Conference*; 2016.

Yu, S.; Fan, Y.; Shi, Z.; Li, J.; Zhao, X.; Zhang, T.; Chang, Z. Hydrogen-based combined heat and power systems: A review of technologies and challenges. 2023.

Chertkov, M.; Novitsky, N. N. Thermal Transients in District Heating Systems. *Energy* **2019**, *184*, 22–33.

Laakkonen, L.; Korpela, T.; Kaivosoja, J.; Vilkko, M.; Majanne, Y.; Nurmoranta, M. Predictive Supply Temperature Optimization of District Heating Networks Using Delay Distributions. Energy Procedia. 2017; pp 297–309.

Zheng, J.; Zhou, Z.; Wang, J.; Hu, S. Research on dynamic thermal characteristics of district heating systems based on return temperatures at heat sources. *Applied Thermal Engineering* **2022**, *214*.

Harmelink, M. *Duurzaamheid van warmte-& koudelevering Voorstel voor inhoud van de rapportageverplichting onder de Warmtewet*.

Aydinalp-Koksal, M.; Ugursal, V. I. Comparison of neural network, conditional demand analysis, and engineering approaches for modeling end-use energy consumption in the residential sector. **2007**,

Gu, W.; Wu, Z.; Bo, R.; Liu, W.; Zhou, G.; Chen, W.; Wu, Z. Modeling, planning and optimal energy management of combined cooling, heating and power microgrid: A review.

Sarbu, I.; Mirza, M.; Crasmareanu, E. A review of modelling and optimisation techniques for district heating systems. 2019.

Olsthoorn, D.; Haghighat, F.; Mirzaei, P. A. Integration of storage and renewable energy into district heating systems: A review of modelling and optimization. 2016.

KRZYSZTOF BADYDA Mathematical model for digital simulation of steam turbine set dynamics and on-line turbine load distribution. *TRANSACTIONS OF THE INSTITUTE OF FLUID-FLOW MACHINERY* **2014**, *126*.

Szapajko, G.; Rusinowski, H. Mathematical modelling of steam-water cycle with auxiliary empirical functions application. *Archives of Thermodynamics* **2010**, *31*, 165–183.

Oppelt, T.; Urbaneck, T.; Gross, U.; Platzer, B. Dynamic thermo-hydraulic model of district cooling networks. *Applied Thermal Engineering* **2016**, *102*, 336–345.

Brange, L.; Englund, J.; Sernhed, K.; Thern, M.; Lauenburg, P. Bottlenecks in district heating systems and how to address them. Energy Procedia. 2017; pp 249–259.

Siddiqui, S.; Macadam, J.; Barrett, M. The operation of district heating with heat pumps and thermal energy storage in a zero-emission scenario. *Energy Reports* **2021**, *7*, 176–183.

Dahash, A.; Steingrube, A.; Ochs, F.; Elci, M. Optimization of District Heating Systems: European Energy Exchange Price-Driven Control Strategy for Optimal Operation of Heating Plants. Proceedings of the 13th International Modelica Conference, Regensburg, Germany, March 4–6, 2019. 2019; pp 169–178.

Viana, A.; Pedroso, J. P. A new MILP-based approach for unit commitment in power production planning. **2012**,

Lahdelma, R.; Hakonen, H. An efficient linear programming algorithm for combined heat and power production. *European Journal of Operational Research* **2003**, *148*, 141–151.

Wang, H.; Yin, W.; Abdollahi, E.; Lahdelma, R.; Jiao, W. Modelling and optimization of CHP based district heating system with renewable energy production and energy storage. *Applied Energy* **2015**, *159*, 401–421.

Coimbra Mills *Basic Heat and Mass transfer*, 3rd ed.; 2015.

Remer Process equipment, cost scale-up. **1993**,

Benalcazar, P.; Kamiński, J. *Mathematical Modelling of Contemporary Electricity Markets*; Elsevier, 2021; pp 237–258.

Benalcazar, P. Optimal sizing of thermal energy storage systems for CHP plants considering specific investment costs: A case study. *Energy* **2021**, *234*.

Sinha, R.; Bak-Jensen, B.; Pillai, J. R.; Zareipour, H. Flexibility from electric boiler and thermal storage for multi energy system interaction. *Energies* **2019**, *13*.

Colophon

This document was typeset using LaTeX, using the KOMA-Script class `scrbook`. The main font is Palatino.